PROBING THE ELECTROWEAK SYMMETRY BREAKING SECTOR WITH THE TOP QUARK**

F. Larios[a,b], E. Malkawi[c] and C.-P. Yuan[a]

[a] Department of Physics and Astronomy, Michigan State University
East Lansing, Michigan 48824 , USA
[b] Departmento de Física, CINVESTAV
Apdo. Postal 14-700, 07000 México, D.F., México
[c] Dept. of Physics, Jordan University of Science I& Technology
P.O. Box 3030-IRBID-22110, Jordan.

(Received September 23, 1996)

A study on the effective anomalous interactions, up to dimension 5, of the top quark with the electroweak gauge bosons is made in the non-linear Chiral Lagrangian approach. Bounds on the anomalous dimension four terms are obtained from their contribution to low energy data. Also, the potential contribution to the production of top quarks at hadron colliders (the Tevatron and the LHC) and the electron Linear Collider from both dimension 4 and 5 operators is analyzed.

PACS numbers: 14.65. Ha, 12.39. Fe, 12.60. -i

1. Introduction

Despite the unquestionable significance of its achievements, like that of predicting the existence of the top quark [1], there is no reason to believe that the Standard Model (SM) is the final theory. For instance, the SM contains many arbitrary parameters with no apparent connections. In addition, the SM provides no satisfactory explanation for the symmetry-breaking mechanism which takes place and gives rise to the observed mass spectrum of the gauge bosons and fermions. Because the top quark is heavy relative

** Presented at the XXXVI Cracow School of Theoretical Physics, Zakopane, Poland, June 1–11, 1996.

to other observed fundamental particles, [1] one expects that any underlying theory; to supersede the SM at some high energy scale $\Lambda \gg m_t$, will easily reveal itself at lower energies through the effective interactions of the top quark to other light particles. Also because the top quark mass ($\sim v/\sqrt{2}$) is of the order of the Fermi scale $v = (\sqrt{2}G_F)^{-1/2} = 246\,\mathrm{GeV}$, which characterizes the electroweak symmetry-breaking scale, the top quark system could be a useful probe for the symmetry-breaking sector. Since the fermion mass generation can be closely related to the electroweak symmetry-breaking, one expects some residual effects of this breaking to appear in accordance with the mass hierarchy [2, 3, 4]. This means that new effects should be more apparent in the top quark sector than in any other light sector of the theory. Therefore, it is important to study the top quark system as a direct tool to probe new physics effects [5].

Many attempts to offer alternative scenarios for the electroweak symmetry breaking mechanism are discussed in literature. A general trend among all alternatives is that new physics appear at or below the TeV scale. Examples include Supersymmetry models [6], technicolor models [6, 7] and possibly extended technicolor sectors to account for the fermion masses [8, 9]. Other examples include top-mode condensate models [10] and a strongly interacting Higgs sector [11].

An attempt to study the nonuniversal interactions of the top quark has been carried out in Ref. [2, 4] by Peccei *et al.* However, in that study only the vertex t-t-Z was considered based on the assumption that this is the only vertex which gains a significant modification due to a speculated dependence of the coupling strength on the fermion mass: $\kappa_{ij} \leq \mathcal{O}\left(\sqrt{m_i m_j}/v\right)$, where κ_{ij} parameterizes some new dimensional–four interactions among gauge bosons and fermions i and j. However, this is not the only possible pattern of interactions, *e.g.*, in some extended technicolor models [9] one finds that the nonuniversal residual interactions associated with the vertices $b_{\rm L}$-$\overline{b_{\rm L}}$-Z , $t_{\rm L}$-$\overline{t_{\rm L}}$-Z , and $t_{\rm L}$-$\overline{b_{\rm L}}$-W to be of the same order.

Because of the great diversity of models proposed for possible new physics (beyond the SM), it has become necessary to be able to study these possible new interactions in a model independent approach [12]. This approach has proved to render relevant non-trivial information about the possible deviations from the standard couplings of the heavier elementary particles (heavy scalar bosons, the bottom and the top quarks, *etc.*) [13]. Our study focuses on the top quark, which because of its remarkably higher

[1] As of the summer of 1996, the mass of the top quark has been measured at the Fermilab Tevatron to be $m_t = 175.6 \pm 5.7\,(\mathrm{stat.}) \pm 7.1(\mathrm{sys.})\,\mathrm{GeV}$ by the CDF group and $m_t = 169 \pm 8\,(\mathrm{stat.}) \pm 8(\mathrm{sys.})\,\mathrm{GeV}$ by the DØ group, through the detection of $t\bar{t}$ events.

mass is the best candidate (among the fermion particles) for manifesting these anomalous interactions at high energies [14].

A common approach to study these anomalous couplings is by considering the most general on-shell vertices (form factors) involving the bottom and the top quarks together with the interaction bosons [5]. In this work we will incorporate the effective chiral Lagrangian approach [15, 16], which is based on the principle of gauge symmetry, but the symmetry is realized in the most general (non-linear) form so as to encompass all the possible interactions consistent with the existing experimental data. The idea of using this approach is to exploit the linearly realized $\mathrm{U}(1)_{\mathrm{em}}$ symmetry and the non-linearly realized $\mathrm{SU}(2)_{\mathrm{L}} \times \mathrm{U}(1)_{\mathrm{Y}}$ symmetry to make a systematic characterization of all the anomalous couplings. In this way, for example, different couplings which otherwise would be considered as independent become related through the equations of motion.

We show that in general low energy data (including Z pole physics) do not impose any stringent constraints on the anomalous dimension four coefficients κ of $\mathcal{L}^{(4)}$ (see Eq. (32)) [2]. This means that low energy data do not exclude the possibility of new physics whose effects come in through the deviations from the standard interactions of the top quark, and these deviations have to be directly measured via production of top quarks at the colliders. For instance, the couplings $\kappa_{\mathrm{L,R}}^{\mathrm{CC}}$ can be measured from the decay of the top quarks in $t\bar{t}$ pairs produced either at hadron colliders (the Fermilab Tevatron and the CERN Large Hadron Collider (LHC)) or at the electron linear collider (LC). They can also be studied from the production of the single-top quark events via, for example, W-gluon or W-photon fusion process [17]. The coupling $\kappa_{\mathrm{L,R}}^{\mathrm{NC}}$ can only be sensitively probed at a future linear collider via the $e^+ e^- \to \gamma, Z \to t\bar{t}$ process because at hadron colliders the $t\bar{t}$ production rate is dominated by QCD interactions ($q\bar{q}, gg \to t\bar{t}$). However, at the LHC $\kappa_{\mathrm{L,R}}^{\mathrm{NC}}$ may also be studied via the associated production of $t\bar{t}$ with Z bosons (this requires a separate study).

Also, we will include the next higher order dimension 5 fermionic operators and then examine the precision with which the coefficients of these operators can be measured in high energy collisions. Since it is the electroweak symmetry breaking sector that we are interested in, we shall concentrate on the interaction of the top quark with the longitudinal weak gauge bosons; which are equivalent to the would-be-Goldstone bosons in the high energy limit. This equivalence is known as the Goldstone Equivalence Theorem [18–21].

[2] For simplicity, we will only construct the complete set of dimension 4 and 5 effective operators for the fermions t and b, although our results can be trivially extended for the other fermion fields, *e.g.* flavor changing neutral interactions t-c-Z, *etc.*

Our strategy for probing these anomalous dimension 5 operators ($\mathcal{L}^{(5)}$) is to study the production of $t\bar{t}$ pairs as well as single-t or $\bar{t}$ via the $W_{\rm L}W_{\rm L}$, $Z_{\rm L}Z_{\rm L}$ and $W_{\rm L}Z_{\rm L}$ (denoted in general as $V_{\rm L}V_{\rm L}$) processes in the TeV region. As we shall show later, based on a power counting method [22], the leading contribution of the scattering amplitudes at high energy goes as E^3 for the anomalous operators $\mathcal{L}^{(5)}$, where $E = \sqrt{s}$ is the CM energy of the WW or ZZ system (that produces $t\bar{t}$), or the WZ system (that produces $t\bar{b}$ or $b\bar{t}$). On the other hand, when the κ coefficients are set equal to zero the dimension 4 operators $\mathcal{L}^{(4)}$ can at most contribute with the first power E^1 to these scattering $V_{\rm L}V_{\rm L}$ processes . In other words, the high energy $V_{\rm L}V_{\rm L} \to f\bar{f}$ scatterings are more sensitive to $\mathcal{L}^{(5)}$ than to $\mathcal{L}^{(4)}$ (with κ's $= 0$). If the κ's are not set equal to zero, then the high energy behaviour can at most grow as E^2 as compared to E^3 for the dimension 5 operators [23]. Furthermore, the dimension 4 anomalous couplings κ's are better measured at the scale of M_W or m_t by studying the decay or the production of the top quark at either the Tevatron and the LHC as mentioned before, or the LC at the $t\bar{t}$ threshold (for the study of Z-t-t).

We show that there are 19 independent dimension 5 operators (with only t, b and gauge boson fields) in $\mathcal{L}^{(5)}$ after imposing the equations of motion for the effective chiral lagrangian. The coefficients of these operators can be measured at either the LHC or the LC to magnitudes of order 10^{-2} or 10^{-1} after normalizing (the coefficients) with the factor [3] $\frac{1}{\Lambda}$ based on the naive dimensional analysis [24, 16]. It is expected that at the LHC or the LC there will be about a few hundreds to a few thousands of $t\bar{t}$ pairs or single-t or single-$\bar{t}$ events produced via the $V_{\rm L}V_{\rm L}$ fusion process.

This work is organized as follows: In Section 2 we will introduce the basic framework of the non-linearly realized chiral Lagrangian, in which the $SU(2)_{\rm L}\times U(1)_{\rm Y}$ gauge symmetry is nonlinearly realized. In this approach, only the $U(1)_{\rm EM}$ symmetry remains unbroken and thus the realization under this subgroup is linear as usual. We will set up a Lagrangian with dimension 4 terms that will reproduce the couplings of the Standard Model type, as well as possible deviations. Then, in Sections 3 and 4 we discuss the constraints on the dimension 4 anomalous couplings from low energy data and the strategies to directly measure these couplings at the hadron or electron colliders. In Sections 5 and 6 we construct the complete set of dimension 5 couplings and discuss their effects to the production of top quarks in high energy regime via weak boson fusion processes. Finally our conclusions are given in Section 7.

---

[3] Λ is the cut-off scale of the effective theory. It could be the lowest new heavy mass scale, or something around $4\pi v \simeq 3.1$ TeV if no new resonances exist below Λ.

2. The non-linearly realized electroweak chiral Lagrangian

We consider the electroweak theories in which the gauge symmetry $G \equiv \mathrm{SU(2)_L} \times \mathrm{U(1)_Y}$ is spontaneously broken down to $H = \mathrm{U(1)}_{em}$[25, 26, 27]. There are three Goldstone bosons, ϕ^a $(a = 1, 2, 3)$, generated by this breakdown of G into H, which are eventually *eaten* by the $W^{\pm}$ and Z gauge bosons and become their longitudinal degrees of freedom.

In the non-linearly realized chiral Lagrangian formulation, the Goldstone bosons transform non-linearly under G but linearly under the subgroup H. A convenient way to implement this is to introduce the matrix field

$$\Sigma = \exp\left(i\frac{\phi^a \tau^a}{v_a}\right) , \tag{1}$$

where τ^a, $a = 1, 2, 3$, are the Pauli matrices normalized as $\mathrm{Tr}(\tau^a \tau^b) = 2\delta_{ab}$. The matrix field Σ transforms under G as

$$\Sigma \to \Sigma' = g_{\mathrm{L}} \Sigma\, g_{\mathrm{R}}^{\dagger} , \tag{2}$$

with

$$\begin{aligned} g_{\mathrm{L}} = & \ \exp\left(i\frac{\alpha^a \tau^a}{2}\right) , \\ g_{\mathrm{R}} = & \ \exp(i\frac{y\tau^3}{2}) , \end{aligned} \tag{3}$$

where $\alpha^{1,2,3}$ and y are the group parameters of G. Because of the $\mathrm{U(1)}_{em}$ invariance, $v_1 = v_2 = v$ in Eq. (1), but they are not necessarily equal to v_3. In the SM, v $(= 246\,\mathrm{GeV})$ is the vacuum expectation value of the Higgs boson field, and characterizes the scale of the symmetry-breaking. Also, $v_3 = v$ arises from the approximate custodial symmetry present in the SM. It is this symmetry that is responsible for the tree-level relation

$$\rho = \frac{M_W^2}{M_Z^2 \cos^2\theta_W} = 1 \tag{4}$$

in the SM, where θ_W is the electroweak mixing angle, M_W and M_Z are the masses of $W^{\pm}$ and Z boson, respectively. In this study we assume the underlying theory guarantees that $v_1 = v_2 = v_3 = v$.

In the context of this non-linear formulation of the electroweak theory, the massive charged and neutral weak bosons can be defined by means of the *composite* field:

$$\mathcal{W}_\mu^a = -i\mathrm{Tr}(\tau^a \Sigma^{\dagger} D_\mu \Sigma) , \tag{5}$$

where [4]

$$D_\mu \Sigma = \left(\partial_\mu - ig\frac{\tau^a}{2}W_\mu^a\right)\Sigma \ . \tag{6}$$

Here, W_μ^a is the gauge boson associated with the $\mathrm{SU}(2)_\mathrm{L}$ group, and its transformation is the usual one (g is the gauge coupling).

$$\tau^a W_\mu^a \to \tau^a W'^a_\mu \ = \ g_\mathrm{L}\, \tau^a W_\mu^a \, g_\mathrm{L}^\dagger \ + \ \frac{2i}{g} g_\mathrm{L} \partial_\mu g_\mathrm{L}^\dagger \, . \tag{7}$$

The $D_\mu \Sigma$ term transforms under G as

$$D_\mu \Sigma \to D_\mu \Sigma' = g_\mathrm{L}\left(D_\mu \Sigma\right) g_\mathrm{R}^\dagger + g_\mathrm{L} \Sigma \partial_\mu g_\mathrm{R}^\dagger \ . \tag{8}$$

Therefore, by using the commutation rules for the Pauli matrices and the fact that $\mathrm{Tr}\,(AB) = \mathrm{Tr}\,(BA)$ we can prove that the composite field $\mathcal{W}_\mu^a$ will transform under G in the following manner:

$$\mathcal{W}_\mu^3 \to \mathcal{W}'^3_\mu = \mathcal{W}_\mu^3 - \partial_\mu y \, , \tag{9}$$

$$\mathcal{W}_\mu^\pm \to \mathcal{W}'^\pm_\mu = e^{\pm iy} \mathcal{W}_\mu^\pm \ , \tag{10}$$

where

$$\mathcal{W}_\mu^\pm = \frac{\mathcal{W}_\mu^1 \mp i\mathcal{W}_\mu^2}{\sqrt{2}} \, . \tag{11}$$

Also, it is convenient to define the field

$$\mathcal{B}_\mu = g' B_\mu \ , \tag{12}$$

which is really the same gauge boson field associated with the $\mathrm{U}(1)_\mathrm{Y}$ group. (g' is the gauge coupling.) The field $\mathcal{B}_\mu$ transforms under G as

$$\mathcal{B}_\mu \to \mathcal{B}'_\mu = \mathcal{B}_\mu + \partial_\mu y \ . \tag{13}$$

We now introduce the composite fields $\mathcal{Z}_\mu$ and $\mathcal{A}_\mu$ as

$$\mathcal{Z}_\mu = \mathcal{W}_\mu^3 + \mathcal{B}_\mu \ , \tag{14}$$

$$s_w^2 \mathcal{A}_\mu = s_w^2 \mathcal{W}_\mu^3 - c_w^2 \mathcal{B}_\mu \, , \tag{15}$$

where $s_w^2 \equiv \sin^2\theta_W$, and $c_w^2 = 1 - s_w^2$. In the unitary gauge ($\Sigma = 1$)

$$\mathcal{W}_\mu^a = -gW_\mu^a \ , \tag{16}$$

[4] This is not the covariant derivative of Σ. The covariant derivative is $D_\mu \Sigma = \partial_\mu \Sigma - ig\frac{\tau^a}{2} W_\mu^a \Sigma + ig'\Sigma\frac{\tau^3}{2} B_\mu$.

$$\mathcal{Z}_\mu = -\frac{g}{c_w} Z_\mu \ , \tag{17}$$

$$\mathcal{A}_\mu = -\frac{e}{s_w^2} A_\mu \ , \tag{18}$$

where we have used the relations $e = gs_w = g'c_w$, $W^3_\mu = c_w Z_\mu + s_w A_\mu$, and $B_\mu = -s_w Z_\mu + c_w A_\mu$. In general, the composite fields contain Goldstone boson fields:

$$\begin{aligned} \mathcal{Z}_\mu &= -\frac{g}{c_w} Z_\mu + \frac{2}{v}\partial_\mu \phi^3 + \cdots, \\ \mathcal{W}^\pm_\mu &= -gW^\pm_\mu + \frac{2}{v}\partial_\mu \phi^\pm + \cdots. \end{aligned} \tag{19}$$

The transformations of $\mathcal{Z}_\mu$ and $\mathcal{A}_\mu$ under G are

$$\mathcal{Z}_\mu \to \mathcal{Z}'_\mu = \mathcal{Z}_\mu \, , \tag{20}$$

$$\mathcal{A}_\mu \to \mathcal{A}'_\mu = \mathcal{A}_\mu - \frac{1}{s_w^2}\partial_\mu y \ . \tag{21}$$

Hence, under G the fields $\mathcal{W}^\pm_\mu$ and $\mathcal{Z}_\mu$ transform as vector fields, but $\mathcal{A}_\mu$ transforms as a gauge boson field which plays the role of the photon field A_μ.

Using the fields defined as above, one may construct the $\mathrm{SU(2)_L \times U(1)_Y}$ gauge invariant interaction terms in the chiral Lagrangian

$$\begin{aligned} \mathcal{L}^B = &- \frac{1}{4g^2}\mathcal{W}^a_{\mu\nu}\mathcal{W}^{a\mu\nu} - \frac{1}{4g'^2}\mathcal{B}_{\mu\nu}\mathcal{B}^{\mu\nu} \\ &+ \frac{v^2}{4}\mathcal{W}^+_\mu \mathcal{W}^{-\mu} + \frac{v^2}{8}\mathcal{Z}_\mu \mathcal{Z}^\mu + \ldots, \end{aligned} \tag{22}$$

where

$$\mathcal{W}^a_{\mu\nu} = \partial_\mu \mathcal{W}^a_\nu - \partial_\nu \mathcal{W}^a_\mu + \varepsilon^{abc}\mathcal{W}^b_\mu \mathcal{W}^c_\nu \, , \tag{23}$$

$$\mathcal{B}_{\mu\nu} = \partial_\mu \mathcal{B}_\nu - \partial_\nu \mathcal{B}_\mu \, , \tag{24}$$

and where ... denotes other possible four- or higher-dimension operators [28, 29].

It is easy to show that [5]

$$\mathcal{W}^a_{\mu\nu}\tau^a = -g\Sigma^\dagger W^a_{\mu\nu}\tau^a \Sigma \tag{25}$$

and

$$\mathcal{W}^a_{\mu\nu}\mathcal{W}^{a\mu\nu} = g^2 W^a_{\mu\nu} W^{a\mu\nu} \, . \tag{26}$$

---

[5] Use $\mathcal{W}^a_\mu \tau^a = -2i\Sigma^\dagger D_\mu \Sigma$, and $[\tau^a, \tau^b] = 2i\varepsilon^{abc}\tau^c$.

This simply reflects the fact that the kinetic term is not related to the Goldstone bosons sector, *i.e.*, it does not originate from the symmetry-breaking sector.

The mass terms in Eq. (22) can be expanded as

$$\frac{v^2}{4}\mathcal{W}^+_\mu \mathcal{W}^{-\mu} + \frac{v^2}{8}\mathcal{Z}_\mu \mathcal{Z}^\mu = \partial_\mu \phi^+ \partial^\mu \phi^- + \frac{1}{2}\partial_\mu \phi^3 \partial^\mu \phi^3 + \frac{g^2 v^2}{4} W^+_\mu W^{\mu -} + \frac{g^2 v^2}{8 c_w^2} Z_\mu Z^\mu + \dots . \quad (27)$$

At the tree-level, the mass of $W^\pm$ boson is $M_W = gv/2$ and the mass of Z boson is $M_Z = gv/2c_w$.

Fermions can be included in this context by assuming that each flavor transforms under $G = \mathrm{SU(2)_L} \times \mathrm{U(1)_Y}$ as [30]

$$f \to f' = \mathrm{e}^{iyQ_f} f\,, \quad (28)$$

where Q_f is the electric charge of f [6].

Out of the fermion fields f_1, f_2 (two different flavors), and the Goldstone bosons matrix field Σ, the usual linearly realized fields Ψ can be constructed. For example, the left-handed fermions [$\mathrm{SU(2)_L}$ doublet] are

$$\Psi_\mathrm{L} \equiv \begin{pmatrix} \psi_1 \\ \psi_2 \end{pmatrix}_\mathrm{L} = \Sigma F_\mathrm{L} = \Sigma \begin{pmatrix} f_1 \\ f_2 \end{pmatrix}_\mathrm{L} \quad (29)$$

with $Q_{f_1} - Q_{f_2} = 1$. One can easily show that Ψ_L transforms linearly under G as

$$\Psi_\mathrm{L} \to \Psi'_\mathrm{L} = \mathrm{g}\Psi_\mathrm{L}\,, \quad (30)$$

where $\mathrm{g} = \exp(i\frac{\alpha^a \tau^a}{2})\exp(iy\frac{Y}{2}) \in G$, and $Y = 1/3$ is the hypercharge of the left handed quark doublet.

In contrast, linearly realized right-handed fermions Ψ_R [$\mathrm{SU(2)_L}$ singlet] simply coincide with F_R, *i.e.*,

$$\Psi_\mathrm{R} \equiv \begin{pmatrix} \psi_1 \\ \psi_2 \end{pmatrix}_\mathrm{R} = F_\mathrm{R} = \begin{pmatrix} f_1 \\ f_2 \end{pmatrix}_\mathrm{R} . \quad (31)$$

With these fields we can now construct the most general gauge invariant chiral Lagrangian that includes the electroweak couplings of the top quark up to dimension four [25] [7].

[6] For instance, $Q_f = 2/3$ for the top quark.

[7] In this study we do not include possible flavor changing neutral current couplings, *e.g.* t-c-Z.

$$
\begin{aligned}
\mathcal{L}^{(4)} = & \; i\bar{t}\gamma^\mu \left(\partial_\mu + i\frac{2s_w^2}{3}\mathcal{A}_\mu\right) t + i\bar{b}\gamma^\mu \left(\partial_\mu - i\frac{s_w^2}{3}\mathcal{A}_\mu\right) b \\
& - \left(\frac{1}{2} - \frac{2s_w^2}{3} + \frac{1}{2}\kappa_{\rm L}^{\rm NC}\right) \overline{t_{\rm L}}\gamma^\mu t_{\rm L}\mathcal{Z}_\mu - \left(\frac{-2s_w^2}{3} + \frac{1}{2}\kappa_{\rm R}^{\rm NC}\right) \overline{t_{\rm R}}\gamma^\mu t_{\rm R}\mathcal{Z}_\mu \\
& - \left(\frac{-1}{2} + \frac{s_w^2}{3}\right) \overline{b_{\rm L}}\gamma^\mu b_{\rm L}\mathcal{Z}_\mu - \frac{s_w^2}{3}\overline{b_{\rm R}}\gamma^\mu b_{\rm R}\mathcal{Z}_\mu \\
& - \frac{1}{\sqrt{2}}\left(1 + \kappa_{\rm L}^{\rm CC}\right) \overline{t_{\rm L}}\gamma^\mu b_{\rm L}\mathcal{W}_\mu^+ - \frac{1}{\sqrt{2}}\left(1 + \kappa_{\rm L}^{\rm CC\dagger}\right) \overline{b_{\rm L}}\gamma^\mu t_{\rm L}\mathcal{W}_\mu^- \\
& - \frac{1}{\sqrt{2}}\kappa_{\rm R}^{\rm CC}\overline{t_{\rm R}}\gamma^\mu b_{\rm R}\mathcal{W}_\mu^+ - \frac{1}{\sqrt{2}}\kappa_{\rm R}^{\rm CC\dagger}\overline{b_{\rm R}}\gamma^\mu t_{\rm R}\mathcal{W}_\mu^- \\
& - m_t\bar{t}t \; .
\end{aligned}
\tag{32}
$$

In the above equation $\kappa_{\rm L}^{\rm NC}$, $\kappa_{\rm R}^{\rm NC}$, $\kappa_{\rm L}^{\rm CC}$, and $\kappa_{\rm R}^{\rm CC}$ parameterize possible deviations from the SM predictions [25, 4]. In general, the charged current coefficients can be complex with the imaginary part introducing a CP odd interaction, and the neutral current coefficients are real so that the effective Lagrangian is Hermitian.

3. Constraints on dimension four anomalous couplings from the low energy data

In the chiral Lagrangian $\mathcal{L}^{(4)}$ given in Eq. (32), there are two complex parameters ($\kappa_{\rm L}^{\rm CC}$ and $\kappa_{\rm R}^{\rm CC}$) and two real ($\kappa_{\rm L}^{\rm NC}$ and $\kappa_{\rm R}^{\rm NC}$) all independent from each other, which need to be constrained using precision data. Naturally, these parameters are not expected to be large, we assume that their absolute values are at most of order one. The imaginary parts of the charged current couplings, which give rise to CP violation at this level, do not contribute to the LEP observables of interest at the one-loop level. Hence, we will ignore imaginary parts of the κ's. Also, at this level any contributions from the right-handed charged current coupling $\kappa_{\rm R}^{\rm CC}$ are proportional to the bottom quark's mass m_b (which is much smaller than m_t), and are negligible compared to the contributions from the other three couplings. Therefore, we can only obtain bounds for $\kappa_{\rm L}^{\rm NC}$, $\kappa_{\rm R}^{\rm NC}$ and $\kappa_{\rm L}^{\rm CC}$ from LEP data at the one loop level. However, the coupling $\kappa_{\rm R}^{\rm CC}$ can be studied independently by using the CLEO measurement of $b \to s\gamma$. For this process $\kappa_{\rm R}^{\rm CC}$ becomes the significant anomalous coupling. In Ref. [31] the contribution of this parameter to the branching ratio of $b \to s\gamma$ was calculated. From the result given there, and the recent CLEO measurement $1\times 10^{-4} < Br(b \to s\gamma) < 4.2\times 10^{-4}$ [32], we can obtain the following bounds for $\kappa_{\rm R}^{\rm CC}$ at the 95% confidence level (C.L.):

$$-0.037 < \kappa_{\rm R}^{\rm CC} < 0.0015 . \tag{33}$$

With these observations we will study how $\kappa_{\rm L}^{\rm NC}$, $\kappa_{\rm R}^{\rm NC}$ and $\kappa_{\rm L}^{\rm CC}$ can be constrained by LEP data.

All contributions to low energy observables, under a few general assumptions, can be parameterized by 4-independent parameters: ε_1, ε_2, ε_3, and ε_b [33, 34, 35]. In our case, the general assumptions are satisfied, namely all the contributions of the non-standard couplings κ's to low energy observables are contained in the oblique corrections, *i.e.*, the vacuum polarization functions of the gauge bosons, and the non-oblique corrections to the vertex b-b-Z. Therefore, it is enough to calculate the new physics contribution to the ε parameters in order to isolate all effects to low energy observables.

The experimental values of the ε parameters are derived from four basic observables, Γ_ℓ (the partial width of Z to a charged lepton pair), A_{FB}^{ℓ} (the forward–backward asymmetry at the Z peak for the charged lepton ℓ), M_W/M_Z, and Γ_b (the partial width of Z to a $b\bar{b}$ pair) [36].

To constrain these nonstandard couplings (κ's) one needs to have the theoretical predictions for the ε's. The SM contribution to the ε's have been calculated in, for example Ref. [37]. Naturally, since we are considering the case of a spontaneous symmetry breaking scenario in which there is no Higgs boson, we have to subtract the Higgs boson contribution from these SM calculations.

Since the top quark will only contribute to the vacuum polarization functions and the vertex b-b-Z, we only need to consider:

$$\varepsilon_1 = e_1 - e_5 , \tag{34}$$
$$\varepsilon_2 = e_2 - c_w^2 e_5 , \tag{35}$$
$$\varepsilon_3 = e_3 - c_w^2 e_5 , \tag{36}$$
$$\varepsilon_b = e_b , \tag{37}$$

where e_1, e_2, e_3, e_5, and e_b are defined as:

$$e_1 = \frac{A^{ZZ}(0)}{M_Z^2} - \frac{A^{WW}(0)}{M_W^2} , \tag{38}$$
$$e_2 = F^{WW}(M_W^2) - F^{33}(M_Z^2) , \tag{39}$$
$$e_3 = \frac{c_w}{s_w} F^{30}(M_Z^2) , \tag{40}$$
$$e_5 = M_Z^2 \frac{dF^{ZZ}}{dq^2}(M_Z^2) . \tag{41}$$

The vacuum polarization functions of the gauge bosons are written in the following form

$$\Pi^{ij}_{\mu\nu}(q^2) = -ig_{\mu\nu}\left(A^{ij}(q^2) + q^2F^{ij}(q^2)\right) + \ q_\mu q_\nu \text{ terms}\,, \tag{42}$$

where $i,j = W,\ Z,\ \gamma$(photon). Alternatively, instead of using Z and γ one can use $i,j = 3,0$ for W^3 and B, respectively. The relation between the two cases is as follows

$$A^{33} = c_w^2 A^{ZZ} + 2s_w c_w A^{\gamma Z} + s_w^2 A^{\gamma\gamma}\,, \tag{43}$$

$$A^{30} = -c_w s_w A^{ZZ} + (c_w^2 - s_w^2)A^{\gamma Z} + c_w s_w A^{\gamma\gamma}\,, \tag{44}$$

$$A^{00} = s_w^2 A^{ZZ} - 2s_w c_w A^{\gamma Z} + c_w^2 A^{\gamma\gamma}\,, \tag{45}$$

and similarly for F^{ij}.

The quantity e_b is defined through the proper vertex correction

$$V_\mu\left(Z \to b\bar{b}\right) = -\frac{g}{2c_w} e_b \gamma_\mu \frac{1-\gamma_5}{2}\,. \tag{46}$$

3.1. Radiative corrections in effective Lagrangians

Before presenting our results for the contributions of the non-standard couplings to the LEP data, we will discuss a key aspect of effective theories in general.

Non–renormalizability of the effective Lagrangian presents a major issue of how to consistently handle both the divergent and the finite pieces in loop calculations [38, 39]. Such a problem arises because one does not know the underlying theory; hence, no matching can be performed to extract the correct scheme to be used in the effective Lagrangian [40]. One approach is to associate the divergent piece in loop calculations with a physical cutoff scale Λ, the upper scale at which the effective Lagrangian is valid [30]. In the chiral Lagrangian approach this cutoff Λ is taken to be $4\pi v \sim 3\,\text{TeV}$ [40] [8]. For the finite piece no completely satisfactory approach is available [38]. We assume that there exists an underlying renormalizable "full" theory that is valid at all scales (or at least at scales much higher than Λ). In this case, Λ serves as an infrared cutoff scale under which the heavy degrees of freedom can be integrated out to give rise to the effective operators in the chiral Lagrangian. Due to the renormalizability of the full

[8] The scale $4\pi v \sim 3\,\text{TeV}$ is only meant to indicate the typical cutoff scale. It is equally probable to have, say, $\Lambda = 1$ TeV.

theory, and from the renormalization group invariance, one concludes that the same cutoff Λ should also serve as the associated ultraviolet cutoff of the effective Lagrangian in the calculation of the Wilson coefficients. Hence, in the dimensional regularization scheme, the ultraviolet divergent piece $1/\varepsilon$ is replaced by $\ln(\Lambda^2/\mu^2)$, where $\varepsilon = (4-n)/2$ and n is the space-time dimension. Furthermore, the renormalization scale μ is set to be m_t, the heaviest mass scale in the low energy effective Lagrangian. To study the effects to low energy observables due to a heavy top quark, in addition to the SM contributions, we shall only include those non-standard contributions (from the κ's) of the order

$$\frac{m_t^2}{16\pi^2 v^2} \ln \frac{\Lambda^2}{m_t^2} . \tag{47}$$

3.2. Contributions on the low energy observables

To perform calculations using the chiral Lagrangian, one should arrange the contributions in powers of $1/4\pi v$ and include all diagrams up to the desired power. In a general R_ξ gauge ($\Sigma \neq 1$), the couplings of the Goldstone bosons to the fermions should also be included in Feynman diagram calculations. These couplings can be easily found by expanding the operators in $\mathcal{L}^{(4)}$.

The relevant Feynman diagrams are shown in figure 1. Calculations can be done for a general R_ξ gauge. As it turns out, the dependence on m_t for ε_1 (which is the deviation from $\rho = 1$) and for ε_b is quadratic, whereas for ε_2 and ε_3 is only logarithmic. Hence, in our effective model, the significant constraints on the parameters $\kappa_{\rm L}^{\rm NC}$, $\kappa_{\rm R}^{\rm NC}$, and $\kappa_{\rm L}^{\rm CC}$ are only coming from ε_1 and ε_b.

The leading contributions (of order $m_t^2 \ln \Lambda^2$) are the following:

- For the vacuum polarization function of the Z boson Fig. 1(a),

$$A^{ZZ}(0) = \frac{M_Z^2}{4\pi^2}\frac{3m_t^2}{v^2}\left(-\kappa_{\rm L}^{\rm NC} + \kappa_{\rm R}^{\rm NC}\right)\frac{1}{\varepsilon} . \tag{48}$$

- For the vacuum polarization function of the W boson Fig. 1(b),

$$A^{WW}(0) = \frac{M_W^2}{4\pi^2}\frac{3m_t^2}{v^2}\left(-\kappa_{\rm L}^{\rm CC}\right)\frac{1}{\varepsilon} . \tag{49}$$

- The vertex corrections are depicted in Figs 1(c), 1(d) and 1(e),

$$(c) \to \frac{ig}{4c_w}\frac{m_t^2}{4\pi^2 v^2}\left(-2\kappa_{\rm L}^{\rm CC}\right)\gamma_\mu\left(1-\gamma_5\right)\frac{1}{\varepsilon} , \tag{50}$$

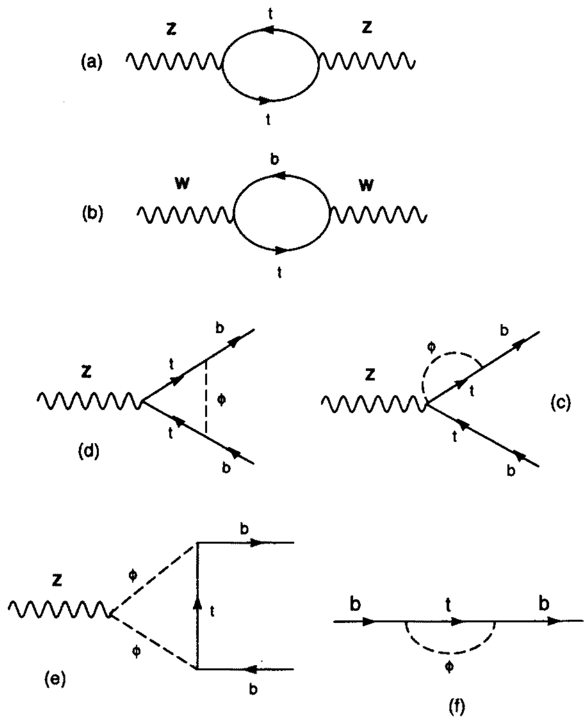

Fig. 1. The relevant Feynman diagrams, for the nonstandard top quark couplings case and in the 't Hooft–Feynman gauge, which contribute to the order $\mathcal{O}(m_t^2 \ln \Lambda^2)$.

- $$(d) \to \frac{ig}{4c_w}\frac{m_t^2}{4\pi^2 v^2}\left(-2c_w^2\kappa_{\rm L}^{\rm CC} + \frac{1}{4}\kappa_{\rm R}^{\rm NC} - \kappa_{\rm L}^{\rm NC}\right)\gamma_\mu\left(1-\gamma_5\right)\frac{1}{\varepsilon}, \qquad (51)$$
- $$(e) \to \frac{ig}{4c_w}\frac{m_t^2}{4\pi^2 v^2}\left(-c_w^2 + \frac{1}{2}\right)\kappa_{\rm L}^{\rm CC}\gamma_\mu\left(1-\gamma_5\right)\frac{1}{\varepsilon}. \qquad (52)$$
- Finally, the b-quark self energy Fig. 1(f) contribution is

$$-\frac{3m_t^2}{16\pi^2 v^2}\gamma_\mu p^\mu\left(\kappa_{\rm L}^{\rm CC}\right)\left(1-\gamma_5\right)\frac{1}{\varepsilon}. \qquad (53)$$

Therefore, the net non-standard contributions to the ε parameters are

$$\delta\varepsilon_1 = \frac{G_F}{2\sqrt{2}\pi^2}3m_t^2(-\kappa_{\rm L}^{\rm NC} + \kappa_{\rm R}^{\rm NC} + \kappa_{\rm L}^{\rm CC})\ln\frac{\Lambda^2}{m_t^2}, \qquad (54)$$

$$\delta\varepsilon_b = \frac{G_F}{2\sqrt{2}\pi^2} m_t^2 \left(-\frac{1}{4}\kappa_{\rm R}^{\rm NC} + \kappa_{\rm L}^{\rm NC}\right) \ln\frac{\Lambda^2}{m_t^2}\,. \tag{55}$$

It is interesting to note that $\kappa_{\rm L}^{\rm CC}$ does not contribute to ε_b up to this order ($m_t^2 \ln \Lambda^2$) which can be understood from Eq. (32). If $\kappa_{\rm L}^{\rm CC} = -1$ then there is no net *t-b-W* coupling in the chiral Lagrangian after including both the standard and nonstandard contributions. Hence, no dependence on the top quark mass can be generated, *i.e.*, the nonstandard $\kappa_{\rm L}^{\rm CC}$ contribution to ε_b must cancel the SM contribution when $\kappa_{\rm L}^{\rm CC} = -1$, independently of the couplings of the neutral current. From this observation and because the SM contribution to ε_b is finite, we conclude that $\kappa_{\rm L}^{\rm CC}$ cannot contribute to ε_b at the order of interest.

Given the above results we can then compare the experimental values of the ε's with the theoretical predictions [41, 42]. For this comparison, we have included all $\varepsilon^{\rm SM}$ and $\delta\varepsilon$, where $\varepsilon^{\rm SM}$ is the SM prediction [9] after subtracting the contributions due to a light Higgs boson (with mass $\sim M_Z$). The other term $\delta\varepsilon$, is the contribution from the dimension 4 anomalous couplings given in Eqs (54) and (55). As we can see, precision data allows for all three non-standard couplings to be different from zero. There is a three dimensional boundary region for these κ's, which we can visualize through the three projections; on the $\kappa_{\rm L}^{\rm CC} = 0$, $\kappa_{\rm R}^{\rm NC} = 0$ and $\kappa_{\rm L}^{\rm NC} = 0$ planes, presented in Figs 2, 3 and 4 respectively. As we can see from the three projections, the only coefficient that is constrained is $\kappa_{\rm L}^{\rm NC}$ which can only vary between -0.5 and 0.5 roughly speaking. The other two can vary through the whole range (-1.0 to 1.0) although in a correlated manner; from figure 4 we can say that LEP data imposes $\kappa_{\rm L}^{\rm CC} \sim -\kappa_{\rm R}^{\rm NC}$ if $\kappa_{\rm L}^{\rm NC}$ is close to zero. This conclusion holds for m_t ranging from 160 GeV to 180 GeV.

In Ref. [2] a similar analysis was done, but in there the anomalous charged current contribution $\kappa_{\rm L}^{\rm CC}$ was not included, and only the non-standard *t-t-Z* couplings were considered. The allowed region they found in Ref. [2] simply corresponds, in our analysis, to the region defined by the intersection of the allowed volume Eq. (54) and the plane $\kappa_{\rm L}^{\rm CC} = 0$, which gives a small area confined in the vicinity of the line $\kappa_{\rm L}^{\rm NC} = \kappa_{\rm R}^{\rm NC}$ (since $\varepsilon_1 \propto \left(\kappa_{\rm R}^{\rm NC} - \kappa_{\rm L}^{\rm NC}\right)$). If we add the restriction given by ε_b Eq. (55), we will realize that this sets the length of the allowed narrow area (*c.f.* Fig. 5).

It is also interesting to consider a special case in which the underlying theory respects the global $SU(2)_{\rm L}\times SU(2)_{\rm R}$ custodial symmetry that is then broken in such a way as to account for a negligible deviation of the *b-b-Z* vertex from its standard form. This scenario will relate the non-standard terms in our effective Lagrangian $\mathcal{L}^{(4)}$ Eq. (32).

---

[9] $\varepsilon^{\rm SM}$ includes also contributions from vertex and box diagrams.

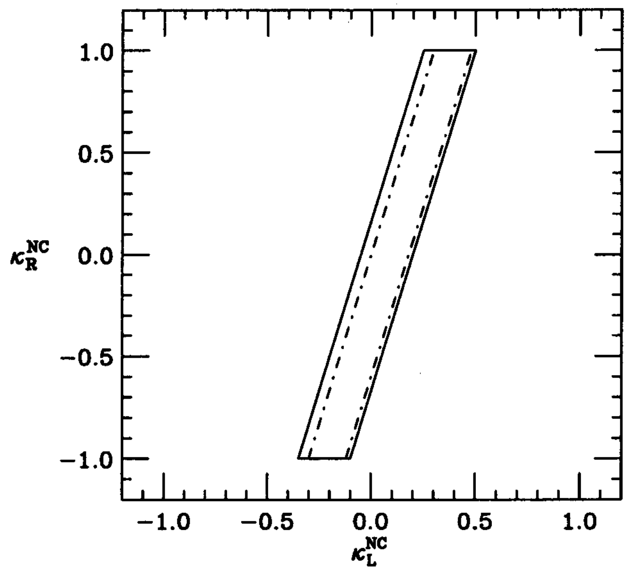

Fig. 2. A two-dimensional projection in the plane of κ_L^{NC} and κ_R^{NC}, for $m_t = 160$ GeV (solid contour) and 180 GeV (dashed contour).

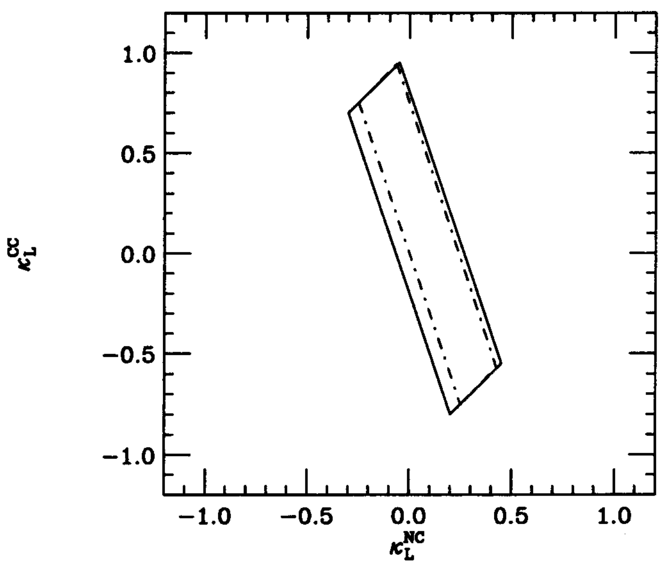

Fig. 3. A two-dimensional projection in the plane of κ_L^{NC} and κ_L^{CC}, for $m_t = 160$ GeV (solid contour) and 180 GeV (dashed contour).

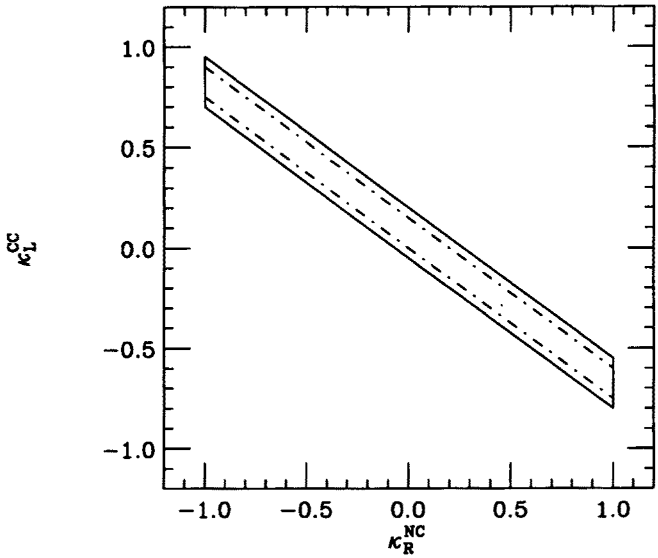

Fig. 4. A two–dimensional projection in the plane of $\kappa_{\rm R}^{\rm NC}$ and $\kappa_{\rm L}^{\rm CC}$, for $m_t = 160$ GeV (solid contour) and 180 GeV (dashed contour).

3.3. Underlying custodial symmetry case

The SM has an additional (accidental) symmetry called the custodial symmetry which is responsible for the tree-level relation [4, 43]

$$\rho = \frac{M_W^2}{M_Z^2\, c_w^2} = 1\,. \tag{56}$$

This symmetry is slightly broken at the quantum level by the SU(2) doublet fermion mass splitting and the hypercharge coupling g' [44]. Writing $\rho = 1 + \delta\rho$, $\delta\rho$ would vanish to all orders if this symmetry were exact. Low energy data indicate that $\delta\rho$ is very close to zero, within about 0.1% accuracy [45].

In the chiral Lagrangian this assumption of a custodial symmetry sets $v_3 = v_2 = v_1$ (see Eq. (1)), and forces the couplings of the top quark to the gauge bosons W_μ^a to be equal after turning off the hypercharge.

Let us consider the case of an underlying global $\mathrm{SU(2)_L \times SU(2)_R}$ symmetry that is broken in such a way as to account for a negligible deviation of the b-b-Z vertex from its standard form. Since the top quark acquires a mass much heavier than the other quarks' masses, we expect the new physics effects associated with the electroweak symmetry breaking (EWSB) sector to be substantially greater for the couplings (to the gauge bosons) of this quark than for the couplings of all the others, including the bottom quark. Therefore, it is natural to think of the initial presence of an underlying theory that respects the custodial symmetry, and then to think of the EWSB mechanism introducing an effective interaction that will explicitly break this symmetry in such a way as to favor the deviation of the couplings of the top quark more than the deviation of the other light quarks' couplings.

In the context of the chiral Lagrangian, let us think of the effective Lagrangian $\mathcal{L}^{(4)}$ Eq. (32) originating from two parts: one that reflects the underlying theory that respects the custodial symmetry (denoted by $\mathcal{L}^{(\text{custodial})}$), and another part that explicitly breaks this symmetry but that keeps the coupling b-b-Z essentially unmodified (denoted by $\mathcal{L}^{(\text{EWSB})}$).

Let us find the most general form for $\mathcal{L}^{(\text{custodial})}$. Notice that if we set $s_w = 0$ (turn off the hypercharge), then the standard $\mathrm{SU}(2)_\mathrm{L}$ invariant term

$$\overline{F_\mathrm{L}}\gamma^\mu \left(i\partial_\mu - \frac{1}{2} \begin{pmatrix} \mathcal{W}^3_\mu & \sqrt{2}\mathcal{W}^+_\mu \\ \sqrt{2}\mathcal{W}^-_\mu & -\mathcal{W}^3_\mu \end{pmatrix} \right) F_\mathrm{L}\,, \tag{57}$$

with the left handed doublets

$$F_\mathrm{L} = \begin{pmatrix} f_1 \\ f_2 \end{pmatrix}_\mathrm{L} \tag{58}$$

defined in Eq. (29), respects the global $\mathrm{SU}(2)_\mathrm{L}\times\mathrm{SU}(2)_\mathrm{R}$ symmetry [10] and is the only structure that does so (the derivative term is trivial). Therefore the only way in which $\mathcal{L}^{(\text{custodial})}$ can contain non-standard couplings is through a term proportional to the same $W^a\tau^a$ structure:

$$\mathcal{L}^{(\text{custodial})} = \overline{F_\mathrm{L}}\gamma^\mu \left(i\partial_\mu - \tfrac{1}{2}\mathcal{W}^a_\mu\tau^a \right) F_\mathrm{L} + \kappa_1 \overline{F_\mathrm{L}}\gamma^\mu \mathcal{W}^a_\mu \tau^a F_\mathrm{L}\,, \tag{59}$$

where κ_1 is a real number (so that $\mathcal{L}^{(\text{custodial})}$ is Hermitian).

Now, for $\mathcal{L}^{(\text{EWSB})}$ we notice that (in the context of the non-linearly realized $\mathrm{SU}(2)_\mathrm{L}\times\mathrm{U}(1)_\mathrm{Y}$ chiral Lagrangian) one can break the custodial symmetry by introducing interaction terms that involve the τ^3 matrix such as

$$\mathcal{L}^{(\text{EWSB})} = \kappa_2 \overline{F_\mathrm{L}}\gamma^\mu \mathcal{W}^a_\mu \tau^a \tau^3 F_\mathrm{L} + \kappa_2^\dagger \overline{F_\mathrm{L}}\gamma^\mu \tau^3 \mathcal{W}^a_\mu \tau^a F_\mathrm{L}\,, \tag{60}$$

where κ_2 is in general a complex number[11].

[10] To verify this, we just need to use the transformation rules $\Sigma \to \Sigma' = L\Sigma R^\dagger$ and $F_\mathrm{L} \to F_\mathrm{L}' = RF_\mathrm{L}$ with R and L members of global $\mathrm{SU}(2)_\mathrm{L}$ and $\mathrm{SU}(2)_\mathrm{R}$ respectively, as well as the identity $i\Sigma^\dagger D_\mu \Sigma = -\mathcal{W}^a_\mu \frac{\tau^a}{2}$.

[11] Another term could be $\overline{F_\mathrm{L}}\gamma^\mu\tau^3\mathcal{W}^a_\mu\tau^a\tau^3 F_\mathrm{L}$, which contains two symmetry breaking factors τ^3. We will not consider this term in our work.

When we add $\mathcal{L}^{(\mathrm{EWSB})}$ to the non-standard part of $\mathcal{L}^{(\mathrm{custodial})}$ we will obtain the term:

$$\overline{F_{\mathrm{L}}}\gamma^{\mu}\begin{pmatrix} (\kappa_1+\kappa_2+\kappa_2^{\dagger})\mathcal{W}_{\mu}^{3} & (\kappa_1-\kappa_2+\kappa_2^{\dagger})\sqrt{2}\mathcal{W}_{\mu}^{+} \\ (\kappa_1+\kappa_2-\kappa_2^{\dagger})\sqrt{2}\mathcal{W}_{\mu}^{-} & (-\kappa_1+\kappa_2+\kappa_2^{\dagger})\mathcal{W}_{\mu}^{3} \end{pmatrix} F_{\mathrm{L}}\,. \tag{61}$$

Therefore, by requiring κ_2 to be a real number, and by setting $\kappa_1 = 2\kappa_2$, the above result indeed describes the scenario in which an underlying custodial symmetric theory is being broken without modifying the coupling b-b-Z from its standard value. By turning the hypercharge back on we will then see that the $\mathcal{L}^{(4)}$ Lagrangian will look like:

$$\mathcal{L}^{(4')} = \overline{F_{\mathrm{L}}}\gamma^{\mu}\left(i\partial_{\mu} - \tfrac{1}{2}\mathcal{W}_{\mu}^{a}\tau^{a}\right)F_{\mathrm{L}} + \overline{F_{\mathrm{L}}}\gamma^{\mu}\kappa_1\begin{pmatrix} 2\mathcal{Z}_{\mu} & \sqrt{2}\mathcal{W}_{\mu}^{+} \\ \sqrt{2}\mathcal{W}_{\mu}^{-} & 0 \end{pmatrix} F_{\mathrm{L}}\,. \tag{62}$$

The superscript $(4')$ in $\mathcal{L}^{(4')}$ is just to differentiate it from the original most general Lagrangian $\mathcal{L}^{(4)}$ of Eq. (32). In conclusion, if we want to consider a special case in which an underlying custodial symmetric theory is being broken by interactions that in the end do not modify the b-b-Z vertex from its standard form, we have to reproduce the matrix structure presented in Eq. (62). This is equivalent to just requiring the relation [12]

$$\kappa_{\mathrm{L}}^{\mathrm{NC}} = 2\kappa_{\mathrm{L}}^{\mathrm{CC}} = 4\kappa_1 \equiv \kappa_{\mathrm{L}} \tag{63}$$

to be satisfied in the original Lagrangian $\mathcal{L}^{(4)}$. Since for the right-handed couplings only the neutral $\kappa_{\mathrm{R}}^{\mathrm{NC}}$ participates in the radiative corrections, we can simplify our notation and set $\kappa_{\mathrm{R}}^{\mathrm{NC}} \equiv \kappa_{\mathrm{R}}$.

From the correlations between the effective couplings (κ's) of the top quark to the gauge bosons, one can infer if the symmetry-breaking sector is due to a model with an approximate custodial symmetry or not, *i.e.*, we may be able to probe the symmetry-breaking mechanism in the top quark system. To illustrate this point, we can compare our results with those in Ref. [2]. Figure 5 shows the most general allowed region for the couplings $\kappa_{\mathrm{L}}^{\mathrm{NC}}$ and $\kappa_{\mathrm{R}}^{\mathrm{NC}}$, *i.e.*, without imposing any "custodial symmetry" relation between $\kappa_{\mathrm{L}}^{\mathrm{NC}}$ and $\kappa_{\mathrm{L}}^{\mathrm{CC}}$. This region is for a top quark mass of 170 GeV and covers the parameter space $-1.0 \le \kappa_{\mathrm{L}}^{\mathrm{NC}}, \kappa_{\mathrm{R}}^{\mathrm{NC}} \le 1.0$. One finds

$$-0.15 \le \kappa_{\mathrm{L}}^{\mathrm{NC}} \le 0.35\,,$$
$$-1.0 \le \kappa_{\mathrm{R}}^{\mathrm{NC}} \le 1.0\,.$$

[12] A relation like this appears in the SM after integrating out an ultra-heavy Higgs boson [4].

We also show in figure 5 the allowed regions for our special case ($\kappa_L^{CC} = {}^1\!/_2\kappa_L^{NC}$) and the model in Ref. [2] $\left(\kappa_L^{CC} = 0\right)$. The two regions overlap in the vicinity of the origin (0, 0) which corresponds to the SM case. Note that for $m_t \leq 200\,\mathrm{GeV}$ the allowed region of κ's in all models of symmetry-breaking should overlap near the origin because the SM is consistent with low energy data at the 95% C.L. For $\kappa_L^{NC} \geq 0.1$, these two regions diverge and become separable. One notices that the allowed range predicted in Ref. [2] lies along the line $\kappa_L^{NC} = \kappa_R^{NC}$ whereas in our case the slope is given by the line $\kappa_L^{NC} = 2\kappa_R^{NC}$.

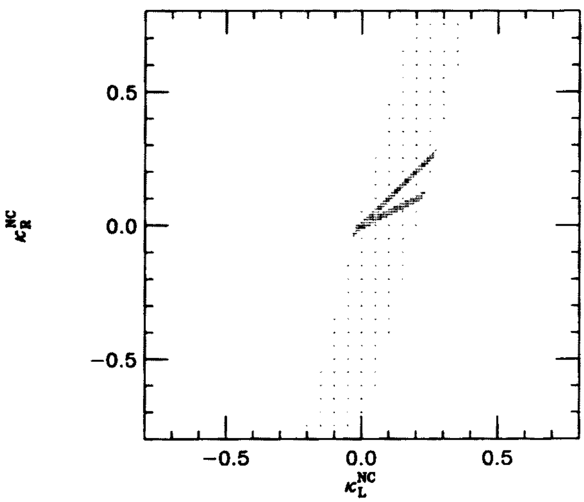

Fig. 5. A comparison between our model and the model in Ref. [2] The allowed regions in both models are shown on the plane of κ_L^{NC} and κ_R^{NC}, for $m_t = 170$ GeV.

If we imagine that any prescribed dependence between the couplings corresponds to a symmetry-breaking scenario, then, given the present status of low energy data, it is possible to distinguish between different scenarios if κ_L^{NC}, κ_R^{NC} and κ_L^{CC} are larger than 10%. Better future measurements of ε's can further discriminate between different symmetry-breaking scenarios with smaller difference in the κ's. Next, we will discuss how the SLC precision data can contribute to the study of the nonstandard couplings.

3.4. At the SLC

The measurement of the left–right cross section asymmetry A_{LR} in Z production with a longitudinally polarized electron beam at the SLC provides a further test of the SM and is sensitive to new physics. The reported measurement of $A_{\rm LR}$ [46] shows a deviation of about 2.8σ from the SM [13] prediction. The effect of the SLC measurement of $A_{\rm LR}$ on possible new physics effects on the top quark couplings depends on the way one incorporates $A_{\rm LR}$ with LEP data. If we include and average $A_{\rm LR}$ with all LEP data, the anomaly in $A_{\rm LR}$ is almost washed away due to the large number of LEP measurements consistent with the SM. One finds that including the SLC measurement $A_{\rm LR}$ with all LEP data yields a slight decrease in the central value of ε_1 [41] while keeping the fit on ε_b the same. As discussed in the previous section, the nonstandard coupling $\kappa_{\rm L}^{\rm NC}$ is mostly constrained by ε_b. Therefore, no significant change in the allowed range of $\kappa_{\rm L}^{\rm NC}$ is expected. The effect of averaging the SLC and LEP data can be easily seen in the special model discussed previously ($\kappa_{\rm L}^{\rm CC} = \kappa_{\rm L}^{\rm NC}/2$). In this case, the length of the allowed area is not affected since it is controlled by ε_b. Since the uncertainty in $\varepsilon_1^{\rm exp.}$ remains almost the same after including the $A_{\rm LR}$ measurement, the width of the allowed area is also hardly modified. The only effect will be to shift the allowed area slightly downward (towards $2\kappa_{\rm R} < \kappa_{\rm L}$). This conclusion is simply due to the preference for a more negative new physics contribution to accommodate the smaller value of $\varepsilon_1^{\rm exp.}$.

We have seen that the precision LEP/SLC data can constrain the couplings $\kappa_{\rm L}^{\rm NC}$, $\kappa_{\rm R}^{\rm NC}$ and $\kappa_{\rm L}^{\rm CC}$, without forcing them to be zero. For $\kappa_{\rm R}^{\rm CC}$ (the right–handed charged current) there is no constraint, because its contribution to the relevant radiative corrections at LEP/SLC is proportional to the bottom quark's mass. However, the nonstandard coupling $\kappa_{\rm R}^{\rm CC}$ can be studied using the $b \to s\gamma$ measurement [31] (*c.f.* Eq. (33)).

The important lesson from the above analysis is that the precision low energy data do not exclude the possibility of having anomalous top quark interactions with the gauge bosons. Also, different models for the electroweak symmetry breaking sector can induce different relations among the κ's. These relations can in turn be used to discriminate between models by comparing their predictions with experimental data. In the next section, we examine how to improve our knowledge of these non-standard couplings by direct measurements at current and future colliders.

4. Direct measurement of dimension four anomalous couplings at colliders

In this Section, we shall discuss how to measure the dimension four anomalous couplings $\kappa_{\rm L}^{\rm NC}$, $\kappa_{\rm R}^{\rm NC}$, $\kappa_{\rm L}^{\rm CC}$, and $\kappa_{\rm R}^{\rm CC}$ at hadron colliders and future electron collider.

Run I at the Fermilab Tevatron (a $\bar{\rm p}$p collider with $\sqrt{S} = 1.8\,{\rm TeV}$) is now complete, and each experiment (CDF and DØ groups) has accumulated an

[13] With a top quark mass $m_t = 175$ GeV and a Higgs mass $m_H = 300$ GeV.

integrated luminosity of about 110 pb^{-1}. Run II (the upgraded Tevatron with the Main Injector) will begin in 1999, with a machine energy of 2 TeV and an integrated luminosity of about 2 fb^{-1} per year. The CERN Large Hadron Collider (LHC) is a pp collider with $\sqrt{S} = 14\,\text{TeV}$ and an integrated luminosity of about 10 $\sim$ 100 fb^{-1} per year. A future electron Linear Collider (LC) is also proposed to run at the top quark pair threshold (via $e^-e^+ \to t\bar{t}$ process) to study the detailed properties of the top quark.

4.1. At the Tevatron and the LHC

At the Tevatron and the LHC, heavy top quarks are predominantly produced in pairs from the QCD process $gg, q\bar{q} \to t\bar{t}$. In addition, there are single-top quark events in which only a single t or $\bar{t}$ is produced. A single-top quark signal can be produced from either the W–gluon fusion process $qg(Wg) \to t\bar{b}$ (or $q'b \to qt$ [47, 48], the Drell–Yan-type W^* process $q\bar{q} \to t\bar{b}$ [45–47] and Wt production via $gb \to W^-t$ [52]. The corresponding Feynman diagrams for these single-top processes are shown in figure 6. The approximate cross sections (in pb) for single-top quark production (including both single-t and single-$\bar{t}$ events) at the upgraded Tevatron (and the LHC) from the above four production processes are 6.5(700), 2.0(200), 0.88(10) and 0.2(70), respectively.

The relative magnitudes between the dimension four anomalous couplings $\kappa_{\rm L}^{\rm CC}$ and $\kappa_{\rm R}^{\rm CC}$ can be measured from the decay of the top quark (produced from either of the above processes) to a bottom quark and a W boson. These nonstandard couplings can be furthered measured from counting the production rates of signal events with a single t or $\bar{t}$. More details can be found in Refs [51], [53] and [54].

4.1.1. From the decay of top quarks

In $t\bar{t}$ events, the final state with most kinematic information is $W + 4j$, where the W is detected via its leptonic decay. These events are fully reconstructable. To reduce backgrounds, it is best to demand at least one b tag. The number of such events is about 500 per fb^{-1} [54]. Thus there will be on the order of 1000 tagged, fully reconstructed top-quark events in Run II, to be compared with the approximately 25 $W + 4j$ single-tagged top events in Run I. To probe $\kappa_{\rm L}^{\rm CC}$ and $\kappa_{\rm R}^{\rm CC}$ from the decay of the top quark to a bottom quark and a W boson, one needs to measure the polarization of the W boson which can be determined by the angular distribution of the lepton (say, e^+ in the rest frame of W^+) in the decay mode $t \to bW^+(\to e^+\nu)$. However, reconstructing the rest frame of the W-boson (in order to measure its polarization) could be a non-trivial matter due to the missing longitudinal momentum (P_Z) (with a two-fold ambiguity) of the neutrino

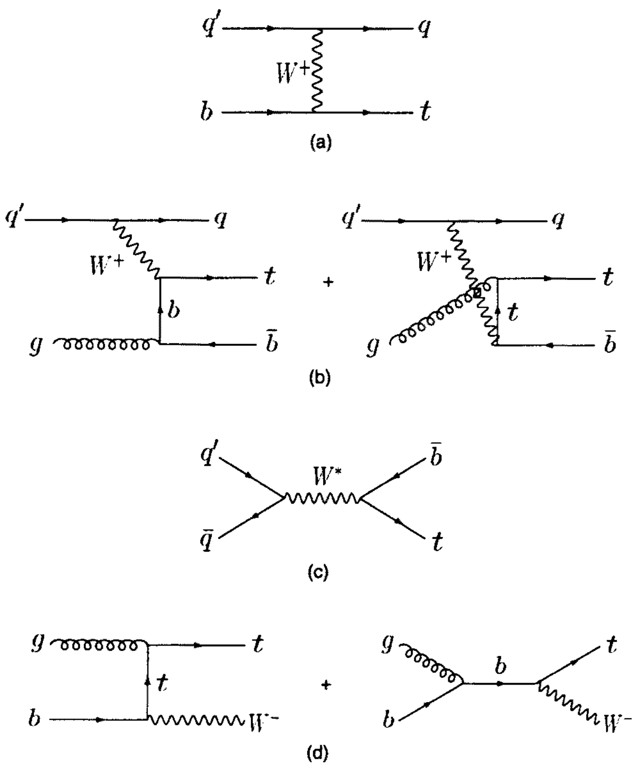

Fig. 6. Diagrams for various single-top quark processes.

(ν) from W decay. Fortunately, as shown in Eq. (64), one can determine the polarization of the W-boson without reconstructing its rest frame by using the Lorentz-invariant observable m_{be}, the invariant mass of b and e from t decay.

The polar angle $\theta^*_{e^+}$ distribution of the e^+ in the rest frame of the W^+ boson whose z-axis is defined to be the moving direction of the W^+ boson in the rest frame of the top quark can be written in terms of m_{be} through the following derivation:

$$\begin{aligned}\cos\theta^*_{e^+} &= \frac{E_e E_b - p_e \cdot p_b}{|\vec{p}_e||\vec{p}_b|} \\ &\simeq 1 - \frac{p_e \cdot p_b}{E_e E_b} = 1 - \frac{2m_{be}^2}{m_t^2 - M_W^2}\,. \end{aligned} \tag{64}$$

The energies E_e and E_b are evaluated in the rest frame of the W^+ boson from the top quark decay and are given by

$$\begin{aligned} E_e &= \frac{M_W^2 + m_e^2 - m_\nu^2}{2M_W}, \qquad |\vec{p}_e| = \sqrt{E_e^2 - m_e^2}, \\ E_b &= \frac{m_t^2 - M_W^2 - m_b^2}{2M_W}, \qquad |\vec{p}_b| = \sqrt{E_b^2 - m_b^2}. \end{aligned} \tag{65}$$

where we have not ignored the negligible masses m_e and m_ν, of e^+ and ν_e, for the sake of book-keeping.

In Eq. (64), the first line comes from exact definition, whereas the second line comes from applying Eq. (65) in the limit $m_b = 0$. However, in practice two problems arise due to experimental limitations. First, the measured momenta of the bottom quark and the charged lepton will be smeared by detector effects, and second; it is difficult to do the identification of the right b to reconstruct t. There are three possible strategies to improve the efficiency of identifying the correct b. One is to demand a large invariant mass of the $t\bar{t}$ system so that t is boosted and its decay products are collimated. Namely, the right b will be moving closer to the lepton from t decay. This can be easily enforced by demanding leptons with a larger transverse momentum. Another strategy is to identify the soft (non-isolated) lepton from the $\bar{b}$ decay (with a branching ratio $\mathrm{Br}(\bar{b} \to \mu^+ X) \sim 10\%$). The third one is to statistically determine the electric charge of the b-jet (or $\bar{b}$-jet) to be $1/3$ (or $-1/3$) [14]. How precisely can the invariant mass m_{be} be measured is a question yet to be answered.

For a massless b (which is a good approximation for $m_b \ll m_t$), the W boson from top quark decay can only be either longitudinally or left-handed polarized for a purely left-handed charged current ($\kappa_{\mathrm{R}}^{\mathrm{CC}} = 0$). For a purely right-handed charged current ($\kappa_{\mathrm{L}}^{\mathrm{CC}} = -1$) the W boson can only be either longitudinally or right-handed polarized. (Note that the handedness of the W boson is reversed for a massless $\bar{b}$ from $\bar{t}$ decays.) This is the consequence of helicity conservation, as diagrammatically shown in figures 7 and 8 for a polarized top quark. In these figures we show the preferred moving direction of the lepton coming from a polarized W-boson decay in the rest frame of a polarized top quark, for both cases of a left-handed and a right-handed t-b-W vertex. As indicated in these figures, the invariant mass $m_{b\ell}$ depends on the polarization of the W-boson from the decay of a polarized top quark. Also, $m_{b\ell}$ is preferentially larger for a purely right-handed t-b-W vertex than for a purely left-handed one. This is clearly shown in figure 9, in which the peak of the $m_{b\ell}$ distribution is shifted to the right

[14] This is the kind of analysis performed at LEP to separate a quark jet from a gluon jet.

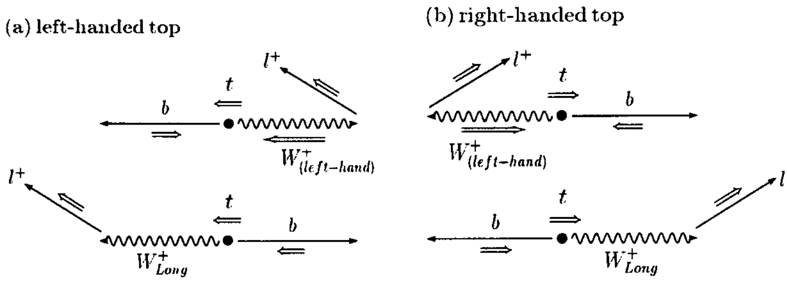

Fig. 7. For a left-handed t-b-W vertex

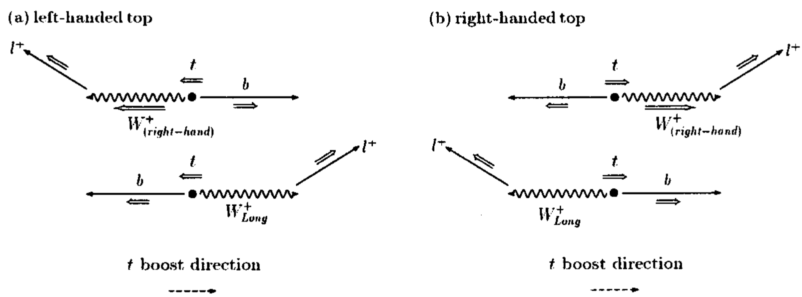

Fig. 8. For a right-handed t-b-W vertex

and the distribution falls off sharply at the upper mass limit for a purely right-handed t-b-W vertex. Their difference is shown, in terms of $\cos\theta^*_\ell$, in figure 10. However, in both cases the fraction ($f_{\rm Long}$) of longitudinal W's from top quark decay is enhanced by ${m_t}^2/2{M_W}^2$ as compared to the fraction of transversely polarized W's [55], namely,

$$f_{\rm Long} = \frac{\frac{m_t^2}{2M_W^2}}{1+\frac{m_t^2}{2M_W^2}} \,. \tag{66}$$

Therefore, for a heavier top quark, it is more difficult to untangle the $\kappa_{\rm L}^{\rm CC}$ and $\kappa_{\rm R}^{\rm CC}$ contributions. [15]

As noted above, studying the decay of the top quark can tell us something about the relative size of the couplings $1+\kappa_{\rm L}^{\rm CC}$ and $\kappa_{\rm R}^{\rm CC}$. To determine the values of $\kappa_{\rm L}^{\rm CC}$ and $\kappa_{\rm R}^{\rm CC}$, one has to provide additional information such as the decay width of $t \to bW^+$ (which is about the total width of the top

[15] On the other hand, because of the very same reason, the mass of a heavy top quark can be accurately measured from $f_{\rm Long}$ irrespective of the nature of the t-b-W couplings (either left-handed or right-handed).

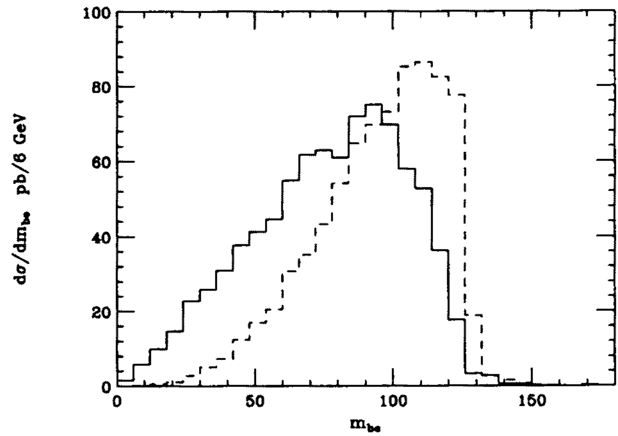

Fig. 9. $m_{b\ell}$ distribution for SM top quark (solid) and for a purely right-handed t-b-W coupling (dash).

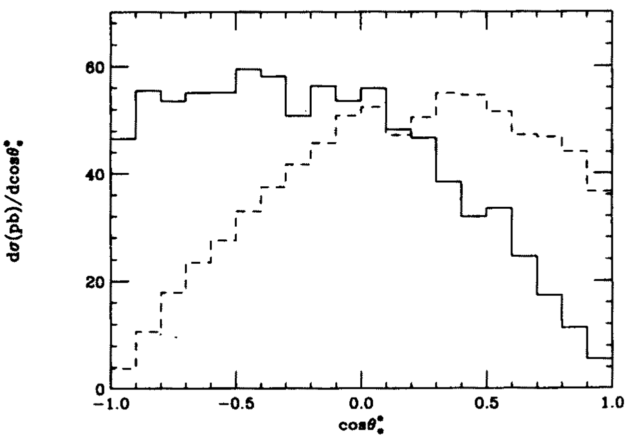

Fig. 10. $\cos\theta^*_\ell$ distribution for SM top quark (solid) and for a purely right-handed t-b-W coupling (dash).

quark in the SM).[16] If we *assume* the decay width of $t \to bW^+$ is the same as the SM prediction (*i.e.*, about 1.5 GeV for a 175 GeV top quark), then the value of $(\kappa_L^{CC})^2 + (\kappa_R^{CC})^2$ is fixed. Thus, combining with the information obtained from the previous analysis one can decisively determine κ_L^{CC} and κ_R^{CC}. The important question to ask then is how to measure the decay width of $t \to bW^+$, denoted as $\Gamma(t \to bW^+)$.

[16] The information (*c.f.* Eq. (33) on κ_R^{CC} derived from the rare-decay process $b \to s\gamma$ could also be useful.

4.1.2. Measuring the decay width of $t \to bW^+$

As shown in Ref. [56], the intrinsic width of the top quark cannot be measured at hadron colliders from reconstructing the invariant mass of the jets from the decay of the top quark produced from the usual QCD processes ($q\bar{q}$, $gg \to t\bar{t}$) because of the poor resolution of the jet energy as measured by the detector. For a 175 GeV SM top quark, its intrinsic width is about 1.5 GeV, however the measured width from the invariant mass distribution of the top quark is unlikely to be much better than 10 GeV [54]. Is there a way to measure the top quark width $\Gamma(t \to bW^+)$ to within a factor of 2 or better, at hadron colliders? The answer is yes. It can be measured from single-top events.

The width $\Gamma(t \to bW^+)$ can be measured by counting the production rate of top quark from the W-b fusion process which is *equivalent* to the W-gluon fusion process by properly treating the bottom quark and the W boson as partons inside the hadron. In the following we shall discuss how to correctly treat the b-quark as a parton inside the proton to properly resum all the large logs to all orders in α_s. First, let us illustrate how to treat the W-boson as a parton inside the proton. Consider the $q'b \to qt$ process. It can be viewed as the production of an on-shell W-boson (*i.e.*, effective-W approximation) which then rescatters with the b-quark to produce the top quark. This factorization is similar to that in the deep-inelastic scattering processes. The analytic expression for the flux ($f_\lambda(x)$) of the incoming W_λ-boson ($\lambda = 0, +, -$ for longitudinal, right-handed, or left-handed polarization) to rescatter with the b-quark can be found in Ref. [57]. The constituent cross section of $ub \to dt$ is given by

$$\hat{\sigma}(ub \to dt) = \sum_{\lambda=0,+,-} f_\lambda \left(x = \frac{m_t^2}{\hat{s}} \right) \left[\frac{16\pi^2 m_t^3}{\hat{s}(m_t^2 - M_W^2)^2} \right] \Gamma(t \to bW_\lambda^+) ,$$

where M_W is the mass of W^+-boson and $\sqrt{\hat{s}}$ is the invariant mass of the hard part process. Note that in order to derive the above result one has to assume that the dynamics of the hard part scattering, *i.e.*, $bW^+(k_\mu) \to t$, does not change dramatically from an off-shell ($k^2 < 0$) to an on-shell ($k^2 = M_W^2$) W-boson. Hence, the above equality is only valid under the effective-W approximation even though the kinematic factors are correctly included. Since the scattering rate of $Wb \to t$ is proportional to the decay rate of $t \to Wb$, the production rate of single-top event from the W-gluon fusion process measures the partial decay width of the top quark $\Gamma(t \to bW^+)$. Furthermore, the branching ratio of $t \to Wb$ can be measured [17] from the ratio of the numbers of double-b-tagged versus single-b-tagged $t\bar{t}$ events

[17] CDF group has reported a measurement of this branching ratio in [58].

and the ratio of $(2\ell + jets)$ and $(1\ell + jets)$ rates in $t\bar{t}$ events for $t \to bW^+(\to \ell^+\nu)$ [54]. Combining this model-independent measurement of the branching ratio $\mathrm{Br}(t \to bW)$ with the measurement of the partial decay width $\Gamma(t \to bW^+)$ from the single-top production rate, one can determine the total decay width $\Gamma_t = \Gamma(t \to bW)/\mathrm{Br}(t \to bW)$ of the top quark, or equivalently, the lifetime $(1/\Gamma_t)$ of the top quark. At the Run-II of the Tevatron we expect that the lifetime of the top quark will be known to about 20% $\sim$ 30%. Here, we have taken the values that the branching ratio $\mathrm{Br}(t \to bW^+)$ can be measured to about 10% [54] and the cross section for W-gluon fusion process is known to about 15% $\sim$ 20% (discussed in the next section).

Before closing this section, we comment on the importance of measuring the single-top production rate from the W-gluon fusion process. In the SM, the only nonvanishing coupling at the tree level is $\kappa_{\rm L}^{\rm CC} = 1$. These κ's would have different values if new physics exists. Nevertheless, the conclusion that the production rate of the W-gluon fusion event is proportional to the decay width of $t \to Wb$ holds irrespective of the specific forms of the anomalous couplings (even including higher order operators). Hence, measuring the single-top event rate from the W-gluon fusion process is an *inclusive* method for detecting effects of new physics which might produce large modifications to the interactions of the top quark. Strictly speaking, from the production rate of single-top events, one measures the sum (weighted by parton densities) of all the possible partial decay widths, such as $\Gamma(t \to bW^+) + \Gamma(t \to sW^+) + \Gamma(t \to dW^+) + \cdots$, therefore, this measurement is actually measuring the width of $\Gamma(t \to XW^+)$ where X can be more than one particle state as long as it originates from the partons inside the proton (or anti-proton). If new physics strongly enhances the flavor-changing-neutral-current t-c-Z, then the single-top production rate would also be enhanced from the Z-c fusion process $qc \to qt$.

4.1.3. The total production rate of W-gluon process

The calculation on the production rate of W-gluon fusion process involves a very important but not yet well-developed technique for handling the kinematics of a *heavy* b parton inside a hadron. Thus, the kinematics of the top quark produced from this process can not be accurately calculated. However, the total event rate of the single-top quark production via this process can be estimated using the method proposed in Ref. [59]. The total rate for W-gluon fusion process involves the $\mathcal{O}(\alpha^2)$ $(2 \to 2)$ process $q'b \to qt$ plus the $\mathcal{O}(\alpha^2\alpha_s)$ $(2 \to 3)$ process $q'g(W^+g) \to qt\bar{b}$ (where the gluon splits to $b\bar{b}$) minus the *splitting* piece $g \to b\bar{b} \otimes q'b \to qt$ in which $b\bar{b}$ are nearly collinear. These processes are shown diagrammatically in figure 11.

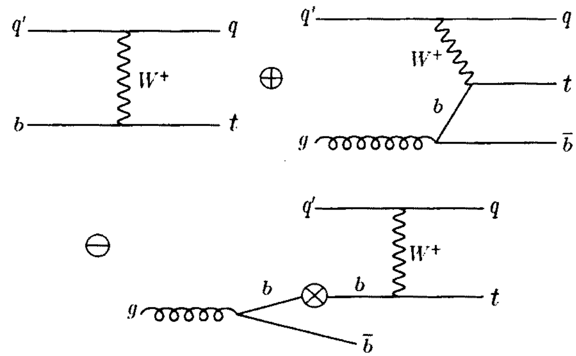

Fig. 11. Feynman diagrams illustrating the subtraction procedure for calculating the total rate for W-gluon fusion: $q'b \to qt \oplus q'g(W^+g) \to qt\bar{b} \ominus (g \to b\bar{b} \otimes q'b \to qt)$.

The splitting piece is subtracted to avoid double counting the regime in which the b propagator in the $(2 \to 3)$ process closes to on-shell. This procedure is to resum the large logarithm $\alpha_s \ln(m_t^2/m_b^2)$ in the W-gluon fusion process to all orders in α_s and include part of the higher order $\mathcal{O}(\alpha^2\alpha_s)$ corrections to its production rate. (m_b is the mass of the bottom quark.) We note that to obtain the complete $\mathcal{O}(\alpha^2\alpha_s)$ corrections beyond just the leading log contributions one should also include virtual corrections to the $(2 \to 2)$ process, but we shall ignore these non-leading contributions in this work[18]. Using the prescription described above we find that when using the $\overline{\text{MS}}$ parton distribution function (PDF) CTEQ2L [61] the total rate of the W-gluon fusion process is about 25% smaller than the $(2 \to 2)$ event rate either at the Tevatron or at the LHC.

To estimate the uncertainty in the production rate due to the choice of the scale Q in evaluating the strong coupling constant α_s and the parton distributions, we show in figure 12 the scale dependence of the W-gluon fusion rate for a SM top quark. As shown in the figure, although the individual rate from either $(2 \to 2)$, $(2 \to 3)$, or the splitting piece is relatively sensitive to the choice of the scale, the total rate as defined by $(2 \to 2)$ + $(2 \to 3)$ – (splitting piece) only varies by about 30% for $M_W/2 < Q < 2m_t$ at the Tevatron. (At the LHC, it varies by about 10%). This uncertainty reduces to about 10% (at the Tevatron) for $m_t/2 < Q < 2m_t$. [19] Based upon the

[18] In Ref. [60] it is shown that indeed these non-leading logs are not important.

[19] This conclusion is in good agreement with a complete next-to-leading-order calculation (different from the above resummation procedure) performed in Ref. [62] in which the theoretical error on the total cross section at the Tevatron was estimated to be about 10% for Q ranging from $m_t/2$ to $2m_t$.

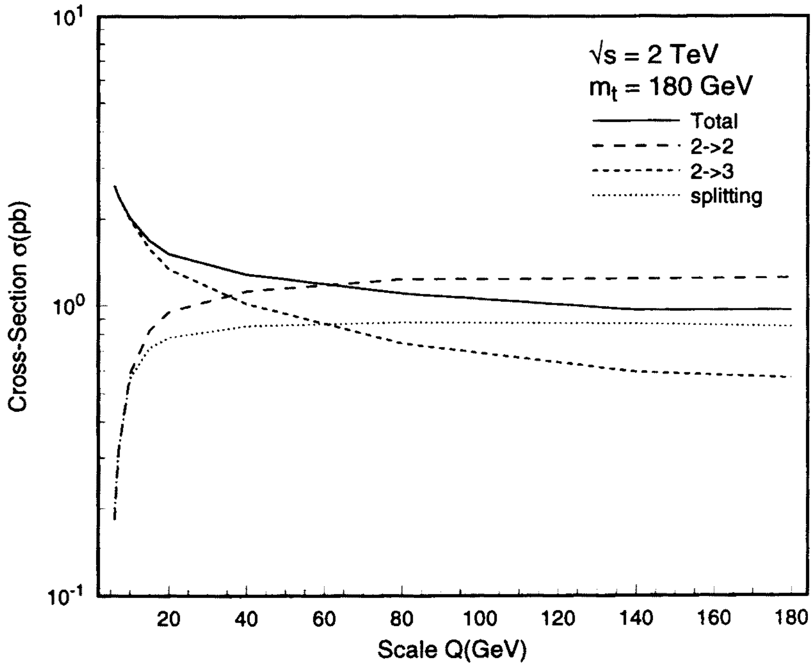

Fig. 12. Rate of W-gluon fusion process versus scale Q for $m_t = 180\,\mathrm{GeV}$ and $\sqrt{s} = 2\,\mathrm{TeV}$.

results shown in figure 12, we argue that $Q < M_W/2$ is probably not a good choice as the relevant scale for the production of the top quark from the W-gluon fusion process because the total rate rapidly increases by about a factor of 2 in the low Q regime. In view of the prescription adopted in calculating the total rate, the only relevant scales are the top quark mass m_t and the virtuality of the W-line in the scattering amplitudes. Since the typical transverse momentum of the quark (q) which comes from the initial quark (q') after emitting the W-line is about half of the W-boson mass, the typical virtuality of the W-line is about $M_W/2 \sim 40\,\mathrm{GeV}$. The scale $m_b \sim 5\,\mathrm{GeV}$ is thus not an appropriate one to be used in calculating the W-gluon fusion rate when using our prescription. We note that in the $(2 \to 2)$ process the b quark distribution effectively contains sums to order $[\alpha_s \ln(Q/m_b)]^n$ from n-fold collinear gluon emission, whereas the subtraction term (namely, the splitting piece) contains only first order in $\alpha_s \ln(Q/m_b)$. Therefore, as $Q \to m_b$ the $(2 \to 2)$ contribution is almost cancelled by the splitting terms. Consequently, as shown in figure 12, the total rate is about the same as the $(2 \to 3)$ rate for $Q \to m_b$. It is easy to see also that based upon the factorization of the QCD theory [59] the total rates calculated via this prescription will not be sensitive to the choice of $\overline{\mathrm{MS}}$ PDF although each individual piece can have different results from different PDF's.

In conclusion, assuming $\kappa_{\mathrm{R}}^{\mathrm{CC}} = 0$, then $\kappa_{\mathrm{L}}^{\mathrm{CC}}$ can be constrained to within $-0.08 < \kappa_{\mathrm{L}}^{\mathrm{CC}} < 0.03$ assuming a 20% uncertainty on the production rate of single-top quark from the W-gluon fusion process at the Tevatron [4]. This means that if we interpret $(1 + \kappa_{\mathrm{L}}^{\mathrm{CC}})$ as the CKM matrix element $|V_{tb}|$, then $|V_{tb}|$ can be bounded as $|V_{tb}| > 0.9$. [20]

4.1.4. Other single-top production rates

Another single-top quark production mechanism is the Drell-Yan type process $q'\bar{q} \to W^* \to t\bar{b}$ whose production rate can also provide information on $\kappa_{\mathrm{L}}^{\mathrm{CC}}$ and $\kappa_{\mathrm{R}}^{\mathrm{CC}}$. Notice that the polarization of the top quark produced from this process is different from the one in W–gluon fusion events [50]. For instance, for a 175 GeV SM top quark produced at the Tevatron, W–gluon fusion produces almost 100% left handed top quarks, but the W^* process produces $\sim$ 50% polarized top quarks (*i.e.*, 1/4 of top quarks are right handed and the rest are left handed). Hence, these production rates depend on $\kappa_{\mathrm{L}}^{\mathrm{CC}}$ and $\kappa_{\mathrm{R}}^{\mathrm{CC}}$ differently. Furthermore, since the kinematics of the top quark produced from these two processes are different [50], these two kinds of events can be separated at the Tevatron. In Ref. [51], a careful study was carried out of how to measure $|V_{tb}|$ from the production rate of W^* events. It was concluded that $|V_{tb}|$ can be measured to about 10% at the Tevatron if $\kappa_{\mathrm{R}}^{\mathrm{CC}} = 0$. It was shown in Ref. [64] that the production rate of W^* events up to the next-to-leading order QCD corrections is well under control (better than 10%). Hence, this process should provide a good measurement of $\kappa_{\mathrm{L}}^{\mathrm{CC}}$ and $\kappa_{\mathrm{R}}^{\mathrm{CC}}$. [21]

We note that because the production cross sections of the single-top events from the W-gluon fusion and the W^* processes depend differently on $\kappa_{\mathrm{L}}^{\mathrm{CC}}$ and $\kappa_{\mathrm{R}}^{\mathrm{CC}}$, they all have to be measured and combined with the measurement of the decay kinematics of the top quark to definitely constrain the anomalous couplings $\kappa_{\mathrm{L}}^{\mathrm{CC}}$ and $\kappa_{\mathrm{R}}^{\mathrm{CC}}$. At the LHC, the single-top production rate from $bg \to Wt$ process is about 7 times the W^* rate and should also be measured to probe the interaction of the top quark with the W-boson.

[20] This method is different from the one used in the recent CDF measurement of $|V_{tb}|$ by measuring $\mathrm{Br}(t \to bW^+)$ and assuming 3 generations of quarks plus unitarity [63]. Our method does not require such assumption.

[21] We note that the production rate of the W^* process is not directly proportional to the decay width of $t \to bW^+$, but the production rate of the W-gluon process is.

4.2. At the LC

The best place to probe the couplings κ_L^{NC} and κ_R^{NC} associated with the t-t-Z coupling is at the LC through $e^-e^+ \to \gamma, Z \to t\bar{t}$ process because at hadron colliders the $t\bar{t}$ production rate is dominated by QCD interactions ($q\bar{q}, gg \to t\bar{t}$). A detailed Monte Carlo study on the measurement of these couplings at the LC including detector effects and initial state radiation can be found in Ref. [65]. The bounds were obtained by studying the angular distribution and the polarization of the top quark produced in e^-e^+ collisions. Assuming a 50 fb^{-1} luminosity at $\sqrt{s} = 500\,\mathrm{GeV}$, we concluded that within a 90% confidence level, it should be possible to measure κ_L^{NC} to within about 8%, while κ_R^{NC} can be known to within about 18%. A 1 TeV machine can do better than a 500 GeV machine in determining κ_L^{NC} and κ_R^{NC} because the relative sizes of the $t_R(\bar{t})_R$ and $t_L(\bar{t})_L$ production rates become small and the polarization of the $t\bar{t}$ pair is purer. Namely, it is more likely to produce either a $t_L(\bar{t})_R$ or a $t_R(\bar{t})_L$ pair. A purer polarization of the $t\bar{t}$ pair makes κ_L^{NC} and κ_R^{NC} better determined. (The degree of top quark polarization can be further improved by polarizing the electron beam [66].) Furthermore, the top quark is boosted more in a 1 TeV machine, thereby allowing a better determination of its polar angle in the $t\bar{t}$ system (because it is easy to find the right b associated with the lepton to reconstruct the top quark moving direction).

Finally, we remark that at the LC κ_L^{CC} and κ_R^{CC} can be studied either from the decay of the top quark pair or from the single–top quark production process, W–photon fusion process $e^-e^+(W\gamma) \to tX$, or $e^-\gamma(W\gamma) \to \bar{t}X$, which is similar to the W–gluon fusion process in hadron collisions.

5. Dimension five anomalous couplings

So far we have discussed how to probe new physics effects that are expected to give some information about the symmetry breaking mechanism, as they can give rise to anomalous terms in the dimension 4 standard gauge couplings of the top quark with the electroweak bosons. Of course, this is not the only way in which these effects can become apparent in future experiments. A complete analysis should include possible anomalous effective interactions of higher dimension. In this section we will construct the complete set of independent operators of the first higher order operators with dimension 5, such that the complete effective Lagrangian relevant to this study will be:

$$\mathcal{L}_{\text{eff}} = \mathcal{L}^B + \mathcal{L}^{(4)} + \mathcal{L}^{(5)}, \tag{67}$$

where $\mathcal{L}^{(5)}$ denotes the dimension 5 operators.

Our next task is to find all the possible dimension five hermitian interactions that involve the top quark and the fields $\mathcal{W}^{\pm}_{\mu}$, $\mathcal{Z}_{\mu}$ and $\mathcal{A}_{\mu}$. Notice that the gauge transformations associated with these and the composite fermion fields Eq. (28) are dictated simply by the $\mathrm{U(1)_{em}}$ group. We will follow a procedure similar to the one in Ref. [67], which consists of constructing all possible interactions that satisfy the required gauge invariance ($\mathrm{U(1)_{em}}$ in this work), and that are not equivalent to each other. The criterion for equivalence is based on the equations of motion and on partial integration. As for the five dimensions in these operators, three will come from the fermion fields, and the other two will involve the gauge bosons. To make a clear and systematic characterization, let us recognize the only three possibilities for these two dimensions:
(1) Operators with two boson fields.
(2) Operators with one boson field and one derivative.
(3) Operators with two derivatives.

(1) **Two boson fields**

First of all, notice that the $\mathcal{A}_{\mu}$ field gauge transformation Eq. (21) will restrict the use of this field to covariant derivatives only. Therefore, except for the field strength term $\mathcal{A}_{\mu\nu}$ only the $\mathcal{Z}$ and $\mathcal{W}$ fields can appear multiplying the fermions in any type of operators. Also, the only possible Lorentz structures are given in terms of the $\sigma_{\mu\nu}$ and $g_{\mu\nu}$ tensors. We do not need to consider the tensor product of γ_{μ}'s since

$$\not a \, \not b = g_{\mu\nu} a_{\mu} b_{\nu} - i\sigma_{\mu\nu} a_{\mu} b_{\nu} \,. \tag{68}$$

Finally, we are left with only three possible combinations: (1.1) two $\mathcal{Z}_{\mu}$'s, (1.2) two $\mathcal{W}_{\mu}$'s, and (1.3) one of each.

1.1 Since $\sigma_{\mu\nu}$ is antisymmetric, only the $g_{\mu\nu}$ part is non-zero [22]:

$$O_{gZZ} = \bar{t}_{\mathrm{L}} t_{\mathrm{R}} \mathcal{Z}_{\mu} \mathcal{Z}^{\mu} + \mathrm{h.c.}. \tag{69}$$

1.2 Here, the antisymmetric part is non-zero too:

$$O_{gWW} = \bar{t}_{\mathrm{L}} t_{\mathrm{R}} \mathcal{W}^{+}_{\mu} \mathcal{W}^{-\mu} + \mathrm{h.c.} \tag{70}$$

$$O_{\sigma WW} = \bar{t}_{\mathrm{L}} \sigma^{\mu\nu} t_{\mathrm{R}} \mathcal{W}^{+}_{\mu} \mathcal{W}^{-}_{\nu} + \mathrm{h.c.} \tag{71}$$

1.3 In this case we have two different quark fields, therefore we can distinguish two different combinations of chiralities:

$$O_{gWZ\mathrm{L(R)}} = \bar{t}_{\mathrm{L(R)}} b_{\mathrm{R(L)}} \mathcal{W}^{+}_{\mu} \mathcal{Z}^{\mu} + \mathrm{h.c.} \tag{72}$$

$$O_{\sigma WZ\mathrm{L(R)}} = \bar{t}_{\mathrm{L(R)}} \sigma^{\mu\nu} b_{\mathrm{R(L)}} \mathcal{W}^{+}_{\mu} \mathcal{Z}_{\nu} + \mathrm{h.c.} \tag{73}$$

[22] In the next section we will write explicitly the Hermitian conjugate (h.c.) parts.

(2) **One boson field and one derivative.**
The obvious distinction arises: (2.1) the derivative acting on a fermion field, and (2.2) the derivative acting on the boson.

2.1 The covariant derivative for the fermions is given by [23] (see Eqs (21) and (28))

$$\begin{aligned} D_\mu f &= (\partial_\mu + iQ_f s_w^2 \mathcal{A}_\mu) f\,, \\ \overline{D_\mu f} &= \bar{f}(\overleftarrow{\partial}_\mu - iQ_f s_w^2 \mathcal{A}_\mu)\,. \end{aligned} \tag{74}$$

Notice that the covariant derivative depends on the fermion charge Q_f, hence the covariant derivative for the top quark is not the same as for the bottom quark; partial integration could not relate two operators involving derivatives on different quarks. Furthermore, by looking at the equations of motion we can immediately see that operators of the form, for example, $\bar{f}\not{\mathcal{Z}}\not{D}f$ or $\bar{f}^{(\mathrm{up})}\not{\mathcal{W}}^{+}\not{D}f^{(\mathrm{down})}$, are equivalent to operators with two bosons, which have all been considered already. Following the latter statement and bearing in mind the identity of Eq. (68) we can see that only one Lorentz structure needs to be considered here, either one with $\sigma_{\mu\nu}$ or one with $g_{\mu\nu}$. Let us choose the latter.

$$O_{\mathcal{W}Db\mathrm{L(R)}} = \mathcal{W}^{+\mu}\bar{t}_{\mathrm{L(R)}} D_\mu b_{\mathrm{R(L)}} + \mathrm{h.c.}\,, \tag{75}$$

$$O_{\mathcal{W}DtR(L)} = \mathcal{W}^{-\mu}\bar{b}_{\mathrm{L(R)}} D_\mu t_{\mathrm{R(L)}} + \mathrm{h.c.}\,, \tag{76}$$

$$O_{\mathcal{Z}Df} = \mathcal{Z}^{\mu}\bar{t}_{\mathrm{L}} D_\mu t_{\mathrm{R}} + \mathrm{h.c.}\,. \tag{77}$$

Of course, the $\mathcal{A}$ field did not appear. Remember that its gauge transformation prevents us from using it on anything that is not a covariant derivative or a field strength $\mathcal{A}_{\mu\nu}$.

2.2 Since $\mathcal{W}$ transforms as a field with electric charge one, the covariant derivative is simply given by (see Eq. (10)):

$$\begin{aligned} D_\mu \mathcal{W}_\nu^+ &= (\partial_\mu + i s_w^2 \mathcal{A}_\mu)\mathcal{W}_\nu^+\,, \\ D_\mu^\dagger \mathcal{W}_\nu^- &= (\partial_\mu - i s_w^2 \mathcal{A}_\mu)\mathcal{W}_\nu^-\,. \end{aligned} \tag{78}$$

Obviously, since the neutral $\mathcal{Z}$ field is invariant under the G group transformations (see Eq. (20)), we could always add it to our covariant derivative:

$$D_\mu^{(\mathcal{Z})}\mathcal{W}_\nu^+ = (\partial_\mu + i s_w^2 \mathcal{A}_\mu + i a \mathcal{Z}_\mu)\mathcal{W}_\nu^+\,,$$

[23] To simplify notation we will use the same symbol D_μ for all covariant derivatives. Identifying which derivative we are referring to should be straightforward, *e.g.* D_μ in Eq. (74) is different from D_μ in Eq. (6).

where a stands for any complex constant. Actually, considering this second derivative would insure the generality of our analysis, since for example by setting $a = c_w^2$ and comparing with Eqs (14) and (15) we would automatically include the field strength term [24]

$$\mathcal{W}^{\pm}_{\mu\nu} = \partial_\mu \mathcal{W}^{\pm}_\nu - \partial_\nu \mathcal{W}^{\pm}_\mu \pm i(\mathcal{W}^{\pm}_\mu \mathcal{W}^3_\nu - \mathcal{W}^3_\nu \mathcal{W}^{\pm}_\mu) = D^{(\mathcal{Z})}_\mu \mathcal{W}^{\pm}_\nu - D^{(\mathcal{Z})}_\nu \mathcal{W}^{\pm}_\mu \tag{79}$$

However, this extra term in the covariant derivative would only be redundant. We can always decompose any given operator written in terms of $D^{(\mathcal{Z})}_\mu$ into the sum of the same operator in terms of the original D_μ plus another operator of the form $O_{g\mathcal{W}\mathcal{Z}\mathrm{L(R)}}$ or $O_{\sigma\mathcal{W}\mathcal{Z}\mathrm{L(R)}}$ (*c.f.* Eqs (72) and (73)). Therefore, we only need to consider the covariant derivative (78) for the charged boson and still maintain the generality of our characterization. For the neutral $\mathcal{Z}$ boson we have the simplest situation, the covariant derivative is just the ordinary one,

$$D_\mu \mathcal{Z}_\nu = \partial_\mu \mathcal{Z}_\nu . \tag{80}$$

The case for the $\mathcal{A}$ boson is nevertheless different. Being the field that makes possible the $\mathrm{U}(1)_{\mathrm{em}}$ covariance in the first place, it can not be given any covariant derivative itself. For $\mathcal{A}$, we have the field strength:

$$\mathcal{A}_{\mu\nu} = \partial_\mu \mathcal{A}_\nu - \partial_\nu \mathcal{A}_\mu ,$$

Finally, we can now write the operators with the covariant derivative-on-boson terms. Unfortunately, no equations of motion can help us reduce the number of independent operators in this case, and we have to bring up both the $\sigma_{\mu\nu}$ and the $g_{\mu\nu}$ Lorentz structures.

$$O_{\sigma D\mathcal{Z}} = \bar{t}_{\mathrm{L}} \sigma^{\mu\nu} t_{\mathrm{R}} \partial_\mu \mathcal{Z}_\nu + \mathrm{h.c.} \tag{81}$$

$$O_{gD\mathcal{Z}} = \bar{t}_{\mathrm{L}} t_{\mathrm{R}} \partial_\mu \mathcal{Z}^\mu + \mathrm{h.c.} \tag{82}$$

$$O_{\sigma D\mathcal{W}L(R)} = \bar{t}_{\mathrm{L(R)}} \sigma^{\mu\nu} b_{\mathrm{R(L)}} D_\mu \mathcal{W}^+_\nu + \mathrm{h.c.} \tag{83}$$

$$O_{gD\mathcal{W}L(R)} = \bar{t}_{\mathrm{L(R)}} b_{\mathrm{R(L)}} D_\mu \mathcal{W}^{+\mu} + \mathrm{h.c.} \tag{84}$$

$$O_{\mathcal{A}} = \bar{t}_{\mathrm{L}} \sigma^{\mu\nu} t_{\mathrm{R}} \mathcal{A}_{\mu\nu} + \mathrm{h.c.} \tag{85}$$

(3) **Operators with two derivatives**

As it turns out, all operators of this kind are equivalent to the ones already given in the previous cases. Here, we shall present the argument of

[24] From Eqs (11) and (23), we write $\mathcal{W}^{\pm}_{\mu\nu} = \frac{1}{\sqrt{2}}(\mathcal{W}^1_{\mu\nu} \mp i\mathcal{W}^2_{\mu\nu})$.

why this is so. First of all, we only have two possibilities, (3.1) one derivative acting on each fermion field, and (3.2) both derivatives acting on the same fermion field.

3.1 Just like in the case (2.1) above, we first notice that an operator of the form $\bar{f}\overleftarrow{\not{D}}\not{D}f$ can be decomposed into operators of the previous cases (1.1), (1.2) and (1.3) by means of the equations of motion. Therefore, we only have to consider one of two options, either $\overline{D_\mu f}\sigma^{\mu\nu}D_\nu f$, or $\overline{D_\mu f}g^{\mu\nu}D_\nu f$. Let us choose the latter. By means of partial integration we can see that the term $(\partial_\mu\bar{f})\partial^\mu f$ yields the same action as the term $-\bar{f}\partial^\mu\partial_\mu f$, and we only need to consider the case in which the covariant derivatives act on the same f, which is just the type of operator to be considered next.

3.2 By using the equations of motion twice we can relate the operator $\bar{f}\not{D}\not{D}f$ to operators of the type (1.1), (1.2) or (1.3). Either $\bar{f}\sigma^{\mu\nu}D_\mu D_\nu f$, or $\bar{f}D^\mu D_\mu f$ needs to be considered. This time we choose the former, which can be proved to be nothing but the operator $O_{\mathcal{A}}$ itself Eq. (92).

5.1. Hermiticity and CP invariance

The list of operators above is complete in the sense that it includes all non-equivalent dimension five interactions that satisfy gauge invariance. It is convenient now to analyze their CP properties. In order to make our study more systematic and clear we will re-write this list again, but this time we will display the added hermitian conjugate part in detail. By doing this the CP transformation characteristics will be most clearly presented too.

Let us divide the list of operators in two: those with only the top quark, and those involving both top and bottom quarks.

5.1.1. Interactions with top quarks only

Let us begin by considering the operator $O_{g\mathcal{Z}\mathcal{Z}}$. We will include an arbitrary constant coefficient, denoted as a, which in principle could be complex:

$$\begin{aligned} O_{g\mathcal{Z}\mathcal{Z}} &= a\bar{t}_{\rm L}t_{\rm R}\mathcal{Z}_\mu\mathcal{Z}^\mu + a^*\bar{t}_{\rm R}t_{\rm L}\mathcal{Z}_\mu\mathcal{Z}^\mu \\ &= \Re(a)\bar{t}t\mathcal{Z}_\mu\mathcal{Z}^\mu + \Im(a)i\bar{t}\gamma_5 t\mathcal{Z}_\mu\mathcal{Z}^\mu\,. \end{aligned}$$

Our hermitian operator has naturally split into two independent parts: one that preserves parity (scalar), and one that does not (pseudoscalar). Also, the first part is CP even whereas the second one is odd. The natural separation of these two parts happens to be a common feature of all operators with only one type of fermion field. Nevertheless, not always will the parity conserving part also be the CP even one, as we shall soon see.

Below, the complete list of all 7 operators with only the top quark is given. In all cases the two independent terms are included; the first one is CP even, and the second one is CP odd.

$$
\begin{aligned}
O_{g\mathcal{Z}\mathcal{Z}} &= \frac{1}{\Lambda}\Re(a_{zz1})\bar{t}t\mathcal{Z}_\mu\mathcal{Z}^\mu + \frac{1}{\Lambda}\Im(a_{zz1})i\bar{t}\gamma_5 t\mathcal{Z}_\mu\mathcal{Z}^\mu\,, && (86)\\
O_{g\mathcal{W}\mathcal{W}} &= \frac{1}{\Lambda}\Re(a_{ww1})\bar{t}t\mathcal{W}^+_\mu\mathcal{W}^{-\mu} + \frac{1}{\Lambda}\Im(a_{ww1})i\bar{t}\gamma_5 t\mathcal{W}^+_\mu\mathcal{W}^{-\mu}\,, && (87)\\
O_{\sigma\mathcal{W}\mathcal{W}} &= \frac{1}{\Lambda}\Im(a_{ww2})i\bar{t}\sigma^{\mu\nu}t\mathcal{W}^+_\mu\mathcal{W}^-_\nu + \frac{1}{\Lambda}\Re(a_{ww2})\bar{t}\sigma^{\mu\nu}\gamma_5 t\mathcal{W}^+_\mu\mathcal{W}^-_\nu\,, && (88)\\
O_{\mathcal{Z}Df} &= \frac{1}{\Lambda}\Im(a_{z3})i\bar{t}D_\mu t\mathcal{Z}^\mu + \frac{1}{\Lambda}\Re(a_{z3})\bar{t}D_\mu\gamma_5 t\mathcal{Z}^\mu\,, && (89)\\
O_{gD\mathcal{Z}} &= \frac{1}{\Lambda}\Im(a_{z4})i\bar{t}\gamma_5 t\partial_\mu\mathcal{Z}^\mu + \frac{1}{\Lambda}\Re(a_{z4})\bar{t}t\partial_\mu\mathcal{Z}^\mu\,, && (90)\\
O_{\sigma D\mathcal{Z}} &= \frac{1}{\Lambda}\Re(a_{z2})\bar{t}\sigma^{\mu\nu}t\partial_\mu\mathcal{Z}_\nu + \frac{1}{\Lambda}\Im(a_{z2})i\bar{t}\sigma^{\mu\nu}\gamma_5 t\partial_\mu\mathcal{Z}_\nu\,, && (91)\\
O_{\mathcal{A}} &= \frac{1}{\Lambda}\Re(a_{\mathcal{A}})\bar{t}\sigma^{\mu\nu}t\mathcal{A}_{\mu\nu} + \frac{1}{\Lambda}\Im(a_{\mathcal{A}})i\bar{t}\sigma^{\mu\nu}\gamma_5 t\mathcal{A}_{\mu\nu}\,. && (92)
\end{aligned}
$$

Notice that in the operator $O_{gD\mathcal{Z}}$ the parity violating part happens to be CP even. This is because under a CP transformation a scalar term $\bar{t}t$ remains intact, *i.e.* it does not change sign, whereas a pseudoscalar term $\bar{t}\gamma_5 t$ changes sign. The gauge bosons change sign too, and this is what makes the scalar part of the operator to change sign under CP. Compare with the operator $O_{g\mathcal{Z}\mathcal{Z}}$, there we have two bosons; two changes of sign that counteract each other. Therefore, it is the scalar part that is CP even in $O_{g\mathcal{Z}\mathcal{Z}}$. Furthermore, based on the naive dimensional analysis (NDA) the coefficients of these operators are of order $1/\Lambda$. Therefore, the normalized coefficients (the a's) are expected to be of order 1.

5.1.2. Interactions with both top and bottom quarks

Below, we show the next list of 12 operators with both top and bottom quarks. Again, we include an arbitrary complex coefficient [25]:

[25] $\overline{D_\mu f}_{\mathrm{R(L)}}$ stands for $(D_\mu f_{\mathrm{R(L)}})^\dagger\gamma_0$; $\bar{f}_{\mathrm{R(L)}}$ stands for $(f_{\mathrm{R(L)}})^\dagger\gamma_0$.

$$\begin{aligned}
O_{g\mathcal{W}\mathcal{Z}\mathrm{L(R)}} &= \frac{1}{\Lambda} a_{wz1L(R)} \bar{t}_{\mathrm{L(R)}} b_{\mathrm{R(L)}} \mathcal{W}^{+}_{\mu} \mathcal{Z}^{\mu} \\
&+ \frac{1}{\Lambda} a^{*}_{wz1L(R)} \bar{b}_{\mathrm{R(L)}} t_{\mathrm{L(R)}} \mathcal{W}^{-}_{\mu} \mathcal{Z}^{\mu} , && (93) \\
O_{\sigma\mathcal{W}\mathcal{Z}\mathrm{L(R)}} &= \frac{1}{\Lambda} a_{wz2L(R)} \bar{t}_{\mathrm{L(R)}} \sigma^{\mu\nu} b_{\mathrm{R(L)}} \mathcal{W}^{+}_{\mu} \mathcal{Z}_{\nu} \\
&+ \frac{1}{\Lambda} a^{*}_{wz2L(R)} \bar{b}_{\mathrm{R(L)}} \sigma^{\mu\nu} t_{\mathrm{L(R)}} \mathcal{W}^{-}_{\mu} \mathcal{Z}_{\nu} , && (94) \\
O_{\mathcal{W}Db\mathrm{L(R)}} &= \frac{1}{\Lambda} a_{bw3L(R)} \mathcal{W}^{+\mu} \bar{t}_{\mathrm{L(R)}} D_{\mu} b_{\mathrm{R(L)}} \\
&+ \frac{1}{\Lambda} a^{*}_{bw3L(R)} \mathcal{W}^{-\mu} \overline{D_{\mu} b}_{\mathrm{R(L)}} t_{\mathrm{L(R)}} , && (95) \\
O_{\mathcal{W}DtR(L)} &= \frac{1}{\Lambda} a_{w3R(L)} \mathcal{W}^{-\mu} \bar{b}_{\mathrm{L(R)}} D_{\mu} t_{\mathrm{R(L)}} \\
&+ \frac{1}{\Lambda} a^{*}_{w3R(L)} \mathcal{W}^{+\mu} \overline{D_{\mu} t}_{\mathrm{R(L)}} b_{\mathrm{L(R)}} , && (96) \\
O_{\sigma D\mathcal{W}L(R)} &= \frac{1}{\Lambda} a_{w2L(R)} \bar{t}_{\mathrm{L(R)}} \sigma^{\mu\nu} b_{\mathrm{R(L)}} D_{\mu} \mathcal{W}^{+}_{\nu} \\
&+ \frac{1}{\Lambda} a^{*}_{w2L(R)} \bar{b}_{\mathrm{R(L)}} \sigma^{\mu\nu} t_{\mathrm{L(R)}} D^{\dagger}_{\mu} \mathcal{W}^{-}_{\nu} , && (97) \\
O_{gD\mathcal{W}L(R)} &= \frac{1}{\Lambda} a_{w4L(R)} \bar{t}_{\mathrm{L(R)}} b_{\mathrm{R(L)}} D_{\mu} \mathcal{W}^{+\mu} \\
&+ \frac{1}{\Lambda} a^{*}_{w4L(R)} \bar{b}_{\mathrm{R(L)}} t_{\mathrm{L(R)}} D^{\dagger}_{\mu} \mathcal{W}^{-\mu} . && (98)
\end{aligned}$$

In this case, if a is real ($a = a^*$) then $O_{g\mathcal{W}\mathcal{Z}\mathrm{L(R)}}$ and $O_{\sigma D\mathcal{W}\mathrm{L(R)}}$ are both CP even, but $O_{\sigma\mathcal{W}\mathcal{Z}\mathrm{L(R)}}$, $O_{\mathcal{W}Db\mathrm{L(R)}}$, $O_{\mathcal{W}Dt\mathrm{R(L)}}$ and $O_{gD\mathcal{W}\mathrm{L(R)}}$ are odd. Just the other way around if a is purely imaginary.

The dimension five Lagrangian $\mathcal{L}^{(5)}$ is simply the sum of all these 19 operators (Eqs (86) to (98)):

$$\mathcal{L}^{(5)} = \sum_{i=1,19} O_i . \qquad (99)$$

To study the possible effects on the production rates of top quarks in high energy collisions, only the CP conserving parts which give imaginary vertices (like the SM) are relevant. The amplitude squared will depend linearly on the CP even terms, but only quadratically on the CP odd terms, because the *no-Higgs* SM ($\mathcal{L}^{(4)}$) interactions [26] are CP even when ignoring

[26] Since in the unitary gauge $\mathcal{L}^{(4)}$ reproduces the SM without the physical Higgs boson, we will refer to it as the *no-Higgs* SM.

the CP-violating phase in the Cabibbo–Kobayashi–Maskawa (CKM) mixing elements.

However, this does not mean that it is not possible to probe the CP violating phase in the operators. Later on in the next section we will show one observable that depends linearly on the CP odd coefficients. From now on, the appropriate CP even part (either real or imaginary) is assumed for each coefficient. To simplify notation we will use the same label; a_{zz1} will stand for $\Re(a_{zz1})$, $a_{wz2L(R)}$ will stand for $\Im(a_{wz2L(R)})$, and so on, the only exception will be $a_{\mathcal{A}}$, whose real part is recognized as proportional to the magnetic moment of the top quark, and will be denoted by a_m. It is thus understood that all coefficients below are real numbers.

In conclusion, the dimension 5 Lagrangian consists of 19 independent operators which are listed from Eq. (86) to Eq. (98). Since the top quark is heavy (its mass is of the order of the weak scale), it is likely to interact strongly with the Goldstone bosons which are equivalent to the longitudinal weak gauge bosons in the high energy regime. (This is known as the Goldstone Equivalence Theorem [21].) Hence, we shall study in the rest of this paper how to probe these anomalous couplings from the production of top quarks via the $V_{\rm L}V_{\rm L}$ fusion process, where $V_{\rm L}$ stands for the longitudinally polarized $W^{\pm}$ or Z bosons.

6. Probing the dimension 5 anomalous couplings at the colliders

As it is suggested by the very form of these operators, we decide to probe their potential contribution to high energy scattering processes like longitudinal vector boson ($V_{\rm L}V_{\rm L}$) fusions (see figure 13), and study how they can affect the production rates of top quarks in both the LHC and the LC. For simplicity, in this study we shall take all the non-standard dimension four couplings to be zero. A general result including these operators are given in Ref. [23].

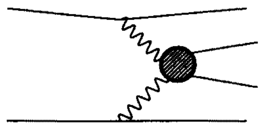

Fig. 13. Production of $t\bar{t}$ ($t\bar{b}$ or $b\bar{t}$) from $W_{\rm L}^+W_{\rm L}^-$ or $Z_{\rm L}Z_{\rm L}$ ($W_{\rm L}^+Z_{\rm L}$ or $W_{\rm L}^-Z_{\rm L}$) fusion processes.

Before doing any calculation at all, we can make an estimate of the expected sizes of these tree level amplitudes according to their high energy behavior. A general power counting rule has been given that estimates the high energy behavior of a scattering amplitude T to be [22]

$$
\begin{aligned}
T &= c_T v^{D_T} \left(\frac{v}{\Lambda}\right)^{N_{\mathcal{O}}} \left(\frac{E}{v}\right)^{D_{E0}} \left(\frac{E}{4\pi v}\right)^{D_{EL}} \left(\frac{M_W}{E}\right)^{e_v} H\left(\ln\frac{E}{\mu}\right), \quad (100) \\
D_{E0} &= 2 + \sum_n \mathcal{V}_n (d_n + \tfrac{1}{2} f_n - 2), \quad D_{EL} = 2L,
\end{aligned}
$$

where $D_T = 4 - e = 0$ (e is the number of external lines; 4 in our case), $N_{\mathcal{O}} = 0$ for all dimension 4 operators and $N_{\mathcal{O}} = 1$ for all dimension 5 operators based upon the naive dimensional analysis (NDA) [27] [24, 16], $L = 0$ is the number of loops in the diagrams, $H(\ln(E/\mu)) = 1$ comes from the loop terms (none in our case), e_v accounts for any external v_μ-lines [28](none in our case of $V_L V_L \to t\bar{t}$, $t\bar{b}$), $\mathcal{V}_n$ is the number of vertices of type n that contain d_n derivatives and f_n fermionic lines. The dimensionless coefficient c_T contains possible powers of gauge couplings (g, g') and Yukawa couplings (y_f) from the vertices of the amplitude T, which can be directly counted.

At high energy the longitudinal components of the gauge bosons will dominate the production of top quarks coming from vector boson fusions, we will thus concentrate on their contribution from now on. According to the Goldstone boson Equivalence Theorem (ET) [21], in the high energy limit we can substitute the longitudinal external weak boson lines with the corresponding Goldstone boson lines, and then perform a much easier calculation. In figure 14 we show these diagrams for the $Z_L Z_L \to t\bar{t}$ process (see also figure 15). Let us start with the *no-Higgs* SM dimension 4 Lagrangian contribution to the process $Z_L Z_L \to t\bar{t}$. It is convenient to use an alternative non-linear parameterization that is equivalent in the sense that it produces the exact same matrix elements [26], but with the advantage that the couplings of the fermions with the Goldstone bosons do not contain derivatives, and we do not have to worry for high energy *gauge* cancellations. The desired form of the SM Lagrangian is given by

$$
\begin{aligned}
\mathcal{L}_{\rm SM}^{(4)} = \; & \overline{\Psi}_{\rm L} i\gamma^\mu D_\mu^L \Psi_{\rm L} + \overline{\Psi}_{\rm R} i\gamma^\mu D_\mu^R \Psi_{\rm R} - \left(\overline{\Psi}_{\rm L} \Sigma M \Psi_{\rm R} + \text{h.c.}\right) \\
& -\frac{1}{4} W^a_{\mu\nu} W^{a\mu\nu} - \frac{1}{4} B_{\mu\nu} B^{\mu\nu} + \frac{v^2}{4} \text{Tr}\left(D_\mu \Sigma^\dagger D^\mu \Sigma\right), \quad (101)
\end{aligned}
$$

[27] NDA counts Σ as Λ^0, D_μ as $1/\Lambda$, and fermion fields as $1/(v\sqrt{\Lambda})$. Hence, $\mathcal{W}^\pm$, $\mathcal{Z}$ and $\mathcal{A}$ are also counted as $1/\Lambda$. After this counting, one should multiply the result by $v^2\Lambda^2$. Notice that up to the order of intent, the kinetic term of the gauge boson fields and the mass term of the fermion fields are two exceptions to the NDA, and are of order Λ^0.

[28] v_μ is equal to $\varepsilon_\mu^{(0)} - \frac{k_\mu}{M_V}$, where k_μ is the momentum of the gauge boson with mass M_V and $\varepsilon_\mu^{(0)}$ is its longitudinal polarization vector.

$$
\begin{aligned}
M &= \begin{pmatrix} m_t & 0 \\ 0 & m_b \end{pmatrix}, \\
D^L_\mu &= \partial_\mu - ig\frac{\tau^a}{2}W^a_\mu - ig'\frac{Y}{2}B_\mu\,, \\
D^R_\mu &= \partial_\mu - ig' Q_f B_\mu\,.
\end{aligned}
$$

In the above equation, $Y = {}^1\!/_3$ is the hypercharge quantum number for the quark doublet, Q_f is the charge of the fermion, $\Psi_{\rm L}$ is the linearly realized left handed quark doublet, and $\Psi_{\rm R}$ is the right handed singlet for top or bottom quarks (see Eqs (29) and (31)). As we have just said, the advantage of using this parameterization for the *no-Higgs* SM case is that once we have made the ET substitution in the diagrams all the high energy cancellations due to gauge boson self-interactions (that have nothing to do with the symmetry breaking sector) will be already taken care of, and we will thus be evaluating directly the high energy behavior of a SM with no Higgs boson.

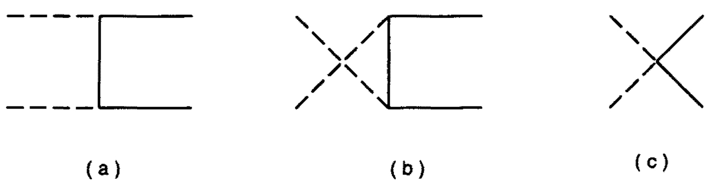

Fig. 14. The corresponding Goldstone boson diagrams for $Z_{\rm L}Z_{\rm L} \rightarrow t\bar{t}$, *i.e.* $\phi^0\phi^0 \rightarrow t\bar{t}$.

When we expand the Σ matrix field up to the second power (see Eq. (1)) in the mass term of Eq. (101), we will notice two things: (*i*) the first power term gives the usual mass term and associates the coefficient $c_T = m_t/v$ to each vertex; (*ii*) the second power term generates the four-point diagram (figure 14(c)) with a coefficient $c_T = m_t^2/v^2$ associated to its vertex. As it is well known, a mass term always involves a chirality flip, therefore we readily recognize that this diagram will only participate when the chiralities of the top and anti-top are different. Since in the high energy regime the mass is much smaller than the energy of the fermions, different chiralities mean equal helicities (for the particle-antiparticle pair). Hence, for the case of opposite helicities we only count the power dependance for diagrams 2(a) and 2(b), and take the highest one. For final state fermions of equal helicities we consider all three diagrams.

The results are the following: for diagrams 2(a) and 2(b) we have $D_{E0} = 2+(-1)+(-1) = 0$, thus the amplitude $T_{\pm\mp}$ is of order m_t^2/v^2; which is the contribution given by the coefficients c_T from both vertices. On the other hand, diagram 2(c) has $D_{E0} = 2 - 1 = 1$; the equal helicities amplitude $T_{\pm\pm}$ will be driven by this dominant diagram, therefore $T_{\pm\pm} = m_t E/v^2$.

For the other processes; $W_L^+ W_L^- \to t\bar{t}$ and $W_L^+ Z_L \to t\bar{b}$, the analysis is the same, except that there is an extra *s-channel* diagram (see figures 16 and 17) that usually behaves just like the four point diagram 14(c).

For the dimension 5 anomalous operators we do not expect *a priori* any *gauge* cancellations at high E. We therefore expect the parameterization used for our effective operators to reflect this high energy behavior. Actually, the chiral lagrangian parameterization given by Eq. (32), which organizes the new physics effects in the momentum expansion [24, 16], is the only framework that allows the existence of such dimension 5 gauge invariant operators. On the other hand, we know that as far as the *no-Higgs* SM contribution to these *anomalous* amplitudes is concerned, it is better to use the equivalent parameterization of Eq. (101), because the right high energy contribution from this model is made easily and consistently. We will therefore use the appropriate couplings from $\mathcal{L}_{\rm SM}^{(4)}$ and $\mathcal{L}^{(5)}$ in our next power counting analysis.

In principle, we can evaluate the contribution to the diagrams 2(a) and 2(b) when both vertices are anomalous, but this would be suppressed by two powers of the cut-off scale; we will just ignore it. We are only considering the contribution from one dimension 5 coupling at a time.

As an example, let us take the operator with derivative on fermion $O_{\mathcal{Z}Df}$ and apply the expansions of the composite fields:

$$\begin{aligned} O_{\mathcal{Z}Df} =& \; a_{z3} i\bar{t} D_\mu t \mathcal{Z}^\mu \\ =& \; -\frac{g}{c_w} a_{z3} i\overline{\psi}_t \partial_\mu \psi_t Z^\mu + \frac{2}{v} a_{z3} i \overline{\psi}_t \partial_\mu \psi_t \partial^\mu \phi^3 + \cdots , \end{aligned} \tag{102}$$

where ψ_t denotes the usual linearly realized top quark field, and $\cdots$ includes the photon field of the covariant derivative, the higher (than zeroth) order terms from the spinor field expansion, and so on. The important thing to notice is that the second term in the right hand side of Eq. (102) is the only one to consider, since all the others either have a lower energy dependance (less derivatives) or do not even represent the effective vertices relevant to the process of interest. Without having to perform similar expansions for all the other operators we can infer that the important effective vertex will always contain two derivatives; the coefficients c_T will be $(2/v)a_O$ for the three-point operators with one derivative on the Goldstone boson field, and $(4/v^2)a_O$ for four-point operators (with two derivatives on the Goldstone boson fields). Nevertheless, two operators are an exception to this rule: $O_{\sigma D\mathcal{Z}}$ and $O_{\sigma D\mathcal{W}L(R)}$. For these operators the *leading* term vanishes; let us expand the second one (for example):

$$a_{w2L(R)}\bar{t}_{\mathrm{L(R)}}\sigma^{\mu\nu}b_{\mathrm{R(L)}}D_\mu W_\nu^+ = -g a_{w2L(R)}\overline{\psi}_{tL(R)}\sigma^{\mu\nu}\psi_{bR(L)}\partial_\mu W_\nu^+ + \frac{2}{v}a_{w2L(R)}\overline{\psi}_{tL(R)}\sigma^{\mu\nu}\psi_{bR(L)}\partial_\mu\partial_\nu\phi^+ + \cdots .$$

As shown, we have the important term vanishing because of the contraction between the antisymmetric $\sigma^{\mu\nu}$ and the symmetric $\partial_\mu\partial_\nu\phi^+$. Hence, this operator will not contribute to the leading high energy behavior for top quark productions via $V_{\mathrm{L}}V_{\mathrm{L}}$ fusion at tree level. It can only contribute to the part of the amplitudes that vanish as $g \to 0$.

As in the previous case of the *no-Higgs* SM, we expect a distinction between the $T_{\pm\mp}$ and $T_{\pm\pm}$ amplitudes. Actually, the situation is the same except for the fact that the anomalous vertex generated by the anomalous operators will yield a $(d_n + {}^1\!/\!_2 f_n - 2) = 1$ factor, whereas the dimension 4 SM operators yield a (-1) factor. Therefore, $D_{E0} = 2 + 1 + (-1) = 0$ for the first two diagrams 2(a) and 2(b) and thus $T_{\pm\mp}$ is of expected to be of order

$$T_{\pm\mp} \sim 2a_O \frac{m_t}{v}\frac{v}{\Lambda}\left(\frac{E}{v}\right)^2 .$$

On the other hand, diagram 2(c) may be generated by either the direct contribution of four-point operators or the contribution from three-point operators when considering higher order terms in their expansion. In each case the anomalous operators contribute with a $(d_n + {}^1\!/\!_2 f_n - 2) = 1$ factor which yields $D_{E0} = 2 + 1 = 3$, and the predicted value for $T_{\pm\pm}$ is

$$T_{\pm\pm} \sim 4a_O \frac{v}{\Lambda}\left(\frac{E}{v}\right)^3 .$$

Naturally, this power counting formula can not predict the fact that sometimes an amplitude can be zero due to the different helicities of spinors. For instance, by performing the calculation of the amplitudes with external gauge bosons in the CM frame we can easily verify that the product of the spinors $\overline{u}_t[\lambda_t = \pm 1]v_{\bar{t}}[\lambda_{\bar{t}} = \mp 1]$ vanishes[29]. This means that contributions from operators of the *scalar*-type, like O_{gZZ}, O_{gWW}, O_{ZDf}, $O_{gWZ\mathrm{L(R)}}$, and $O_{WDtR(L)}$ will vanish for $T_{\pm\mp}$ amplitudes. Also, we have the relation $\varepsilon_\mu p^\mu = 0$ applicable to all three polarizations of external on-shell boson lines, which will make the contribution of operators with derivative on boson and scalar Lorentz contraction like O_{gDZ} and $O_{gDWL(R)}$ to vanish in *t-channel* and *u-channel* diagrams (figure 15). In principle, one would think that the

[29] $u_t[\lambda_t = +1]$ denotes the spinor of a top quark with right handed helicity.

exception could be the *s-channel* type diagram. Actually, this is the case for the operator $O_{gDWL(R)}$ which is able to contribute significantly on the single top production process $W_L^+ Z_L \to t\bar{b}$ (see Table III). However, for the O_{gDZ} operator even this diagram vanishes; as can be easily verified by performing the calculation in the CM frame. One will see that the result of making the Lorentz contraction between the boson propagator $-g_{\mu\nu} + k_\mu k_\nu / M_Z^2$ and the tri-boson coupling is identically zero in the process $W_L^+ W_L^- \to t\bar{t}$. Therefore, for the O_{gDZ} operator all the possible Feynman diagrams vanish, so it does not contribute to the $t\bar{t}$ production rate.

In Tables I, II and III we show the leading contributions (in powers of the CM energy E) of all the operators for each different process; those cells with a dash mean that no anomalous vertex generated by that operator intervenes in the given process, and those cells with a zero mean that the anomalous vertex intervenes in the process but the amplitude vanishes for any of the reasons explained above.

TABLE I

The leading high energy terms for the 4-point operators

Process	$\mathcal{L}^{(4)}$	O_{gZZ} $a_{zz1}\times$	O_{gWW} $a_{ww1}\times$	$O_{\sigma WW}$ $a_{ww2}\times$	$O_{gWZL(R)}$ $a_{wz1L(R)}\times$	$O_{\sigma WZL(R)}$ $a_{wz2L(R)}\times$
$Z_L Z_L \to t\bar{t}$	$m_t E/v^2$	$E^3/v^2\Lambda$	–	–	–	–
$W_L^+ W_L^- \to t\bar{t}$	$m_t E/v^2$	–	$E^3/v^2\Lambda$	$E^3/v^2\Lambda$	–	–
$W_L^+ Z_L \to t\bar{b}$	m_t^2/v^2	–	–	–	$E^3/v^2\Lambda$	$E^3/v^2\Lambda$

TABLE II

The leading high energy terms for the operators with derivative-on-fermion

Process	$\mathcal{L}^{(4)}$	O_{ZDf} $a_{z3}\times$	O_{WDtR} $a_{w3R}\times$	O_{WDtL} $a_{w3L}\times$
$Z_L Z_L \to t\bar{t}$	$m_t E/v^2$	$E^3/v^2\Lambda$	–	–
$W_L^+ W_L^- \to t\bar{t}$	$m_t E/v^2$	$E^3/v^2\Lambda$	$E^3/v^2\Lambda$	$m_b E^2/v^2\Lambda \to 0$
$W_L^+ Z_L \to t\bar{b}$	m_t^2/v^2	$E^3/v^2\Lambda$	$E^3/v^2\Lambda$	$E^3/v^2\Lambda$

TABLE III

The leading high energy terms for the operators with derivative-on-boson

Process	$\mathcal{L}^{(4)}$	O_{gDZ} $a_{z4}\times$	$O_{gDWL(R)}$ $a_{w4}\times$	$O_{\sigma DZ}$ $a_{z2}\times$	$O_{\sigma DWL(R)}$ $a_{w2}\times$	$O_{\mathcal{A}}$ $a_m\times$
$Z_L Z_L \to t\bar{t}$	$m_t E/v^2$	0	–	$g^2 E/\Lambda$	–	–
$W_L^+ W_L^- \to t\bar{t}$	$m_t E/v^2$	0	0	$E^3/v^2\Lambda$	$g^2 E/\Lambda$	$E^3/v^2\Lambda$
$W_L^+ Z_L \to t\bar{b}$	m_t^2/v^2	0	$E^3/v^2\Lambda$	$g^2 E/\Lambda$	$E^3/v^2\Lambda$	–

In conclusion, based on the NDA [24, 16] and the power counting rule [22], we have found that the leading high energy behavior in the $V_L V_L \to t\bar{t}$ *or* $t\bar{b}$ scattering amplitudes from the *no-Higgs* SM operators ($\mathcal{L}^{(4)}_{\rm SM}$) can only grow as $m_t E/v^2$ (for T_{++} or T_{--}, E is the CM energy of the top quark system), whereas the contribution from the dimension 5 operators ($\mathcal{L}^{(5)}$) can grow as $E^3/v^2\Lambda$ in the high energy regime. Let us compare the above results with those of the $V_L V_L \to V_L V_L$ scattering processes. For these $V_L V_L \to V_L V_L$ amplitudes the leading behavior at the lowest order gives E^2/v^2, and the contribution from the next-to-leading order (NLO) bosonic operators gives $(E^2/\Lambda^2)(E^2/v^2)$ [22]. This indicates that the NLO contribution is down by a factor of E^2/Λ^2 in $V_L V_L \to V_L V_L$. On the other hand, the NLO fermionic contribution in $V_L V_L \to t\bar{t}$ *or* $t\bar{b}$ is only down by a factor $E^2/m_t\Lambda$ which compared to E^2/Λ^2 turns out to be bigger by a factor of $(\Lambda/m_t) \sim 4\sqrt{2}\pi$ for $\Lambda \sim 4\pi v$. Hence, we expect that the NLO contributions in the $V_L V_L \to t\bar{t}$ *or* $t\bar{b}$ processes can be better measured (by about a factor of 10) than the $V_L V_L \to V_L V_L$ counterparts for some class of electroweak symmetry breaking models in which the NDA gives reasonable estimates of the coefficients.

As to be shown later, the coefficients of the NLO fermionic operators in $\mathcal{L}^{(5)}$ can be determined via top quark production to order 10^{-2} or 10^{-1}. In contrast, the coefficients of the NLO bosonic operators are usually determined to about an order of 10^{-1} or 1 [21, 68] via $V_L V_L \to V_L V_L$ processes. Therefore, we conclude that the top quark production via the longitudinal gauge boson fusions $V_L V_L \to t\bar{t}$ *or* $t\bar{b}$ at high energy may be more sensitive for probing some symmetry breaking mechanism than the scattering of longitudinal gauge bosons alone ($V_L V_L \to V_L V_L$).

Our next step is to study the production rates of $t\bar{t}$ pairs and single-t or single-$\bar{t}$ events at future colliders like LHC and LC. We will also estimate how accurate these NLO fermionic operators can be measured via the $V_L V_L \to t\bar{t}$ *or* $t\bar{b}$ processes.

6.1. Underlying custodial symmetry

To reduce the number of independent parameters in this study, we shall make the same assumption of an underlying custodial symmetric theory that gets broken in such a way that only the couplings that involve the top quark get modified; as was done for the case of $\mathcal{L}^{(4')}$ (see Eq. (62) and the discussion there). The analysis for the operators with derivatives is exactly the same. The custodial symmetric dimension 5 Lagrangian has the same SU(2) structure [30] as $\mathcal{L}^{(\mathrm{custodial})}$ in Eq. (59):

$$\mathcal{L}^{(\mathrm{5deriv})} = \kappa_{1g}^{(5)}\overline{F_{\mathrm{L}}} g_{\mu\nu} D_\mu \mathcal{W}_\nu^a \tau^a F_{\mathrm{R}} \; + \; \kappa_{1\sigma}^{(5)}\overline{F_{\mathrm{L}}}\sigma^{\mu\nu} D_\mu \mathcal{W}_\nu^a \tau^a F_{\mathrm{R}} \; + \mathrm{h.c.}\,, \qquad (103)$$

and the symmetry breaking term will also be similar to $\mathcal{L}^{(\mathrm{EWSB})}$ in Eq. (60). Therefore the conclusion is the same, that in order to keep the couplings b-b-Z unaltered we have to conform to the matrix structure of $\mathcal{L}^{(4')}$ in Eq. (62), and this will impose the condition

$$a_{z(2,3,4)} = \sqrt{2} a_{w(2,3,4)L(R)} \qquad (104)$$

to all the operators with derivatives.

For the case of 4-point operators the situation is somewhat different. The custodial Lagrangian in this case is of the form:

$$\begin{aligned}
\mathcal{L}^{(\mathrm{5custod})} &= \kappa_{1g}^{\mathrm{4pt.}}\overline{F_{\mathrm{L}}} g^{\mu\nu} \mathcal{W}_\mu^a \tau^a \mathcal{W}_\nu^b \tau^b F_{\mathrm{R}} + \kappa_{1\sigma}^{\mathrm{4pt.}}\overline{F_{\mathrm{L}}}\sigma^{\mu\nu} \mathcal{W}_\mu^a \tau^a \mathcal{W}_\nu^b \tau^b F_{\mathrm{R}} \\
&= \kappa_{1g}^{\mathrm{4pt.}}\overline{F_{\mathrm{L}}} g^{\mu\nu} \begin{pmatrix} \mathcal{W}_\mu^3 \mathcal{W}_\nu^3 + 2\mathcal{W}_\mu^+ \mathcal{W}_\nu^- & 0 \\ 0 & \mathcal{W}_\mu^3 \mathcal{W}_\nu^3 + 2\mathcal{W}_\mu^+ \mathcal{W}_\nu^- \end{pmatrix} F_{\mathrm{R}} \\
&\quad + \kappa_{1\sigma}^{\mathrm{4pt.}}\overline{F_{\mathrm{L}}}\sigma^{\mu\nu} \begin{pmatrix} 2\mathcal{W}_\mu^+ \mathcal{W}_\nu^- & 0 \\ 0 & 2\mathcal{W}_\mu^+ \mathcal{W}_\nu^- \end{pmatrix} F_{\mathrm{R}}\,, \qquad (105)
\end{aligned}$$

and for the symmetry breaking Lagrangian we can consider two terms:

$$\begin{aligned}
\mathcal{L}^{(\mathrm{5EWSB})} &= \sum_{c=g,\sigma} c^{\mu\nu} \Big(\kappa_{2c}^{\mathrm{4pt.}}\overline{F_{\mathrm{R}}}\tau^3 \mathcal{W}_\mu^a \tau^a \mathcal{W}_\nu^b \tau^b F_{\mathrm{L}} + \kappa_{2c}^{\mathrm{4pt.}\dagger}\overline{F_{\mathrm{L}}} \mathcal{W}_\mu^a \tau^a \mathcal{W}_\nu^b \tau^b \tau^3 F_{\mathrm{R}} \\
&\quad + \kappa_{3c}^{\mathrm{4pt.}}\overline{F} \mathcal{W}_\mu^a \tau^a \tau^3 \mathcal{W}_\nu^b \tau^b F \Big)\,, \qquad (106)
\end{aligned}$$

where $\kappa_{3c}^{\mathrm{4pt.}}$ is real and $\kappa_{2c}^{\mathrm{4pt.}}$ is complex. As it turns out, in order to set the anomalous couplings of the bottom quark equal to zero, we have to choose $\kappa_{3c}^{\mathrm{4pt.}} = 0$, and $\kappa_{2c}^{\mathrm{4pt.}}$ real and half the size of $\kappa_{1c}^{\mathrm{4pt.}}$ ($\kappa_{1c}^{\mathrm{4pt.}} = 2\kappa_{2c}^{\mathrm{4pt.}}$ for

[30] Notice that the composite left and right handed doublets $F_{L,R}$ transform in the same way under global $\mathrm{SU}(2)_{\mathrm{R}} \times \mathrm{SU}(2)_{\mathrm{L}}$, $F_{L,R} \to F'_{L,R} = RF_{L,R}$ with R in $\mathrm{SU}(2)_{\mathrm{R}}$.

$c = g, \sigma$). The non-standard 4-point dimension 5 interactions will then have the structure

$$\begin{pmatrix} c^{\mu\nu}\mathcal{W}^3_\mu\mathcal{W}^3_\nu + 2c^{\mu\nu}\mathcal{W}^+_\mu\mathcal{W}^-_\nu & 0 \\ 0 & 0 \end{pmatrix}, \tag{107}$$

where $c^{\mu\nu}$ is either $g^{\mu\nu}$ or $\sigma^{\mu\nu}$.

In conclusion, by assuming that our dimension 5 interactions are the result of an underlying custodial symmetric theory that is broken in such a way that only the couplings of the top quark get modified from the SM values, we can impose the following conditions to the effective coefficients:

$$\begin{aligned} a_{z(2,3,4)} &= \sqrt{2}a_{w(2,3,4)L(R)}, \\ 2a_{zz1} &= a_{ww1}, \\ a_{wz1L(R)} &= a_{wz2L(R)} = 0. \end{aligned} \tag{108}$$

6.2. *Production rates for Z_LZ_L, W_LW_L, and W_LZ_L fusion processes*

Below, we present the helicity amplitudes for each process. We have simplified our analysis as much as possible by considering only the leading terms in powers of E, and by assuming an approximate SU(2) custodial symmetry. As a rule, the next to leading contribution in the E expansion is always two powers down as compared to the leading contribution. Also, the special case of custodial symmetry is assumed in this study; the amplitudes for the most general case are presented elsewhere [23].

6.2.1. $Z_LZ_L \to t\bar{t}$

Comparing with the results for W_LW_L and W_LZ_L fusions, this is the amplitude that takes the simplest form with no angular dependance. This means that any new physics effects coming through this process only modify the S-partial wave amplitude. The notation for the amplitudes indicates the helicity of the outgoing fermions: the first (second) symbol (+ or −) refers to the fermion on top (bottom) part of the diagram. A right handed fermion is labelled by '+', and a left handed fermion by '−' [31]. Figure 15 shows the diagrams that contribute to this process. We take only one anomalous vertex at a time.

The leading contributions to the various helicity amplitudes from the dimension 5 operators are ($E = \sqrt{s}$ is the CM energy of the V_LV_L system):

[31] For example, the anomalous amplitude azz_{++} stands for the anomalous contribution to the amplitude for the production of right handed t and $\bar{t}$ via Z_LZ_L fusion.

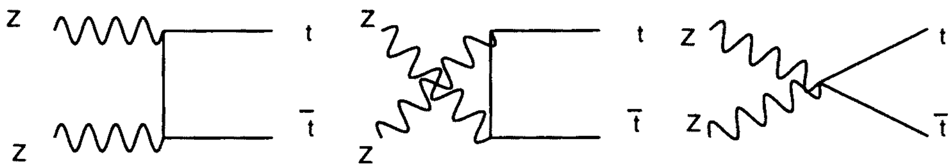

Fig. 15. Diagrams for the $ZZ \to t\bar{t}$ process.

$$\begin{aligned} azz_{++} &= -azz_{--} = -\frac{E^3}{v^2}\frac{X}{\Lambda}, \\ azz_{+-} &= azz_{-+} = 0, \end{aligned} \tag{109}$$

where

$$X = a_{zz1} + \left(\tfrac{1}{2} - \tfrac{4}{3}s_w^2\right) a_{z3}. \tag{110}$$

Notice how at this stage it is impossible to distinguish the effect of the coefficient a_{zz1} from the effect of the coefficient a_{z3}. However, in the next section we will show how we can still combine this information with the results of the other processes, and obtain bounds for each coefficient.

6.2.2. $W_L^+ W_L^- \to t\bar{t}$

The amplitudes of this process are similar to the ones of the previous process except for the presence of two *s-channel* diagrams (see figure 16), whose off-shell γ and Z propagators allow for the contribution from the magnetic moment of the top quark and the operator with derivative on boson $O_{\sigma DZ}$ (a_{z2}), respectively. Also, since these two operators are not of the *scalar*-type, we have a non-zero contribution to the $T_{\pm\mp}$ amplitudes, and an angular dependance that will help in distinguishing the effect of their coefficient X_m from the effect of the coefficient for the *scalar* operators X'. Throughout this study, the angle of scattering θ in all processes is defined to be the one subtended between the center of mass momentum of the incoming gauge boson that appears on the top-left part of the Feynman diagram (W^+ in this case) and the momentum of the outgoing fermion appearing on the top-right part of the same diagram (t in this case).

The leading contributions to the various helicity amplitudes for this process from the dimension 5 operators are:

$$aww_{++} = -aww_{--} = \frac{-2\,E^3}{v^2}\frac{\left(X' + 2X_m c_\theta\right)}{\Lambda},$$

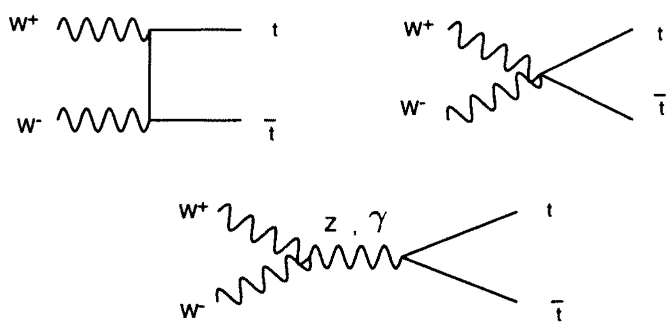

Fig. 16. Diagrams for the $WW \to t\bar{t}$ process.

$$
\begin{aligned}
aww_{-+} &= \frac{8E^2}{v^2} m_t s_\theta \frac{X_m - \frac{1}{8}a_{z3}}{\Lambda}\,, \\
aww_{+-} &= \frac{8E^2}{v^2} m_t s_\theta \frac{\left(X_m - \frac{1}{4}a_{z3}\right)}{\Lambda}\,,
\end{aligned}
\tag{111}
$$

where

$$
\begin{aligned}
X' &= 2a_{zz1} + \tfrac{1}{4}a_{z3}\,, \\
X_m &= a_m - \tfrac{1}{2}a_{z2} + \tfrac{1}{4}a_{z3} + \tfrac{1}{2}a_{ww2}\,.
\end{aligned}
\tag{112}
$$

Notice that the angular distribution of the leading contributions in the $T_{\pm\pm}$ amplitudes consists of the flat component (S-wave) and the $d^1_{0,0} = \cos\theta$ component (P-wave). The $T_{\pm\mp}$ helicity amplitudes only contain the $d^1_{0,\pm 1} = -\sin\theta/\sqrt{2}$ component. This is so because the initial state consists of longitudinal gauge bosons and has zero helicity. The final state is a fermion pair so that the helicity of this state can be -1, 0, or $+1$. Therefore, in high energy scatterings the anomalous dimension 5 operators only modify the leading contributions on the S-type and P-type partial waves of the scattering amplitudes. We also note that, as expected, $T_{\pm\pm}$ has an E^3 leading behavior, whereas $T_{\pm\mp}$ only has an E^2 contribution.

6.2.3. $W_L^+ Z_L \to t\bar{b}$

Finally, we have the amplitudes for the single-top quark production process $W^+Z \to t\bar{b}$ (which are just the same as for the conjugate process $W^-Z \to b\bar{t}$). Figure 17 shows the diagrams that participate in this process.

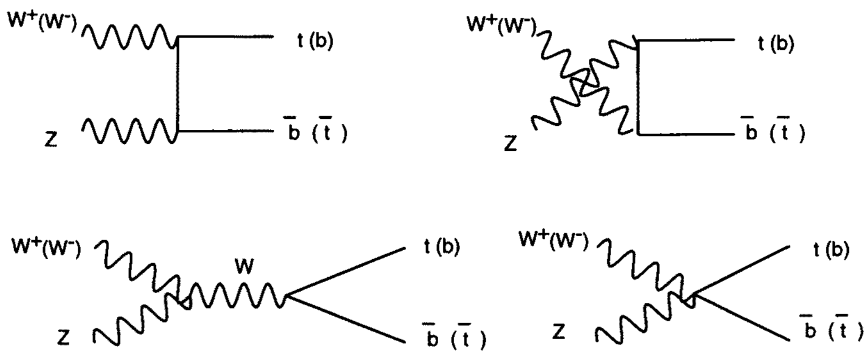

Fig. 17. Diagrams for the $WZ \to t\bar{b}$ process.

The leading contributions to the various helicity amplitudes for this process from the dimension 5 operators are [32]:

$$
\begin{aligned}
awzt_{++} &= \frac{2\sqrt{2}E^3}{v^2}\frac{\left(X_1 - X_2 c_\theta - (\frac{2s_w^2}{3} - 1 - c_\theta)X_3\right)}{\Lambda}\,, \\
awzt_{--} &= \frac{-2\sqrt{2}E^3}{v^2}\frac{\left(X_1 - X_2 c_\theta - (\frac{2s_w^2}{3} + c_\theta - 1)X_3\right)}{\Lambda}\,, \\
awzt_{+-} &= \frac{2\sqrt{2}E^2}{v^2} m_t s_\theta \frac{(X_3 + X_2)}{\Lambda}\,, \\
awzt_{-+} &= \frac{2\sqrt{2}E^2}{v^2} m_t s_\theta \frac{(X_2 - 3X_3)}{\Lambda}\,,
\end{aligned}
\tag{113}
$$

where

$$
\begin{aligned}
X_1 &= \tfrac{1}{2} s_w^2 a_{z4}\,, \\
X_2 &= \tfrac{1}{2} c_w^2 a_{z2}\,, \\
X_3 &= \tfrac{1}{8} a_{z3}\,.
\end{aligned}
\tag{114}
$$

[32] For the approximate custodial symmetry case, the 4-point vertex diagram does not contribute.

Here, as in the previous case, we can distinguish the effect from the three coefficients X_1, X_2, and X_3 by looking at their different angular contribution; X_1's is flat, X_2's and X_3 is in part through s_θ and in part through c_θ.

In order to simplify our numerical analysis we have made the approximation $aww_{+-} \simeq aww_{-+}$. We have verified numerically that the error thus introduced, is of about 5% or less; depending on the difference between X_m and a_{z3} or the value chosen for the angle of scattering θ.

6.3. Top quark production rates from $V_L V_L$ fusions

As discussed above, the top quark productions from $V_L V_L$ fusion processes can be more sensitive to the electroweak symmetry breaking sector than the longitudinal gauge boson productions from $V_L V_L$ fusions. In this section we shall examine the possible increase (or decrease) of the top quark events at the future hadron collider LHC (a pp collider with $\sqrt{s} = 14$ TeV and 100 fb^{-1} of integrated luminosity) and the future electron linear collider LC (an $e^- e^+$ collider with $\sqrt{s} = 1.5$ TeV and 200 fb^{-1} of integrated luminosity) [33].

To simplify our discussion we shall assume an approximate custodial symmetry and use the helicity amplitudes given in the previous section to compute the production rates for $t\bar{t}$ pairs and for single-t or $\bar{t}$ quarks. We shall adopt the effective-W approximation method [17] and use the CTEQ3L parton distribution function with the factorization scale chosen to be the mass of the W-boson [69]. For this study we do not intend to do a detailed Monte Carlo simulation for the detection of the top quark; therefore, we shall only impose a minimal set of cuts on the produced t or b. The rapidity of t or b produced from the $V_L V_L$ fusion process is required to be within 2 (*i.e.* $|y^{t,b}| \leq 2$) and the transverse momentum of t or b is required to be at least 20 GeV. To validate the effective-W approximation, we also require the invariant mass M_{VV} to be larger than 500 GeV.

Since we are working in the high energy regime $E \gg v$, the leading contributions (proportional to E^3) to the $V_L V_L \to t\bar{t}$ *or* $t\bar{b}$ scattering amplitudes that come from the dimension 5 operators in $\mathcal{L}^{(5)}$ and the leading contributions (proportional to E^1) from the *no-Higgs* SM Lagrangian $\mathcal{L}^{(4)}_{\rm SM}$ become a very good approximation.

It is apparent from the helicity amplitudes listed in the previous section that the top quark production rates from $V_L V_L$ fusion depend on a few independent dimension 5 operators. For instance, for $W^\pm_L Z_L$ fusion the

[33] This is another energy phase of the proposed LC.

production rates depend on the combined coefficients ($X1$, $X2$, $X3$), for $W_L^+W_L^-$ fusion depends on (X', X_m), and for Z_LZ_L fusion only depends on (X).

As noted before, in all the $T_{\pm\pm}$ amplitudes, the dimension 5 operators will only modify the constant term (S-wave) and the $\cos\theta$ (P-wave: $d^1_{0,0}$) dependence in the angular distributions for the leading E^3 contributions, whereas all the $T_{\pm\mp}$ amplitudes have a $\sin\theta$ (P-wave: $d^1_{0,\pm1}$) dependence in their leading E^2 contributions. In general, the contributions to these partial waves do not cancel. Hence, let us examine the dependence of the top quark production rates as a function of the coefficients of the operators that only contribute the S-partial wave of the scattering amplitudes. Namely, they are X', X and X_1 for the $W_L^+W_L^-$, Z_LZ_L and $W_L^\pm Z_L$ fusion processes respectively [34]. The predicted top quark event rates as a function of these coefficients are given in Figs 18 and 19 for the LHC and the LC, respectively. In these plots, neither the branching ratio nor the detection efficiency have been included.

The *no-Higgs* SM event rates are given in Figs 18 and 19 for $X = 0$. At the LHC, there are in total about 1500 $t\bar{t}$ pair and single-t or $\bar{t}$ events predicted by the *no-Higgs* SM. The $W_L^+W_L^-$ fusion rate is about a factor of 2 larger than the Z_LZ_L fusion rate, and about an order of magnitude larger than the $W_L^+Z_L$ fusion rate. The $W_L^-Z_L$ rate, which is not shown here, is about a factor of 3 smaller than the $W_L^+Z_L$ rate due to smaller parton luminosities at a pp collider. The large slopes of the $W_L^+W_L^- \to t\bar{t}$ and $Z_LZ_L \to t\bar{t}$ curves, as a function of X indicate that the scattering processes are sensitive enough to probe the anomalous couplings X' and X respectively.

For the LC, because of the small coupling of Z-e-e, the event rate for $Z_LZ_L \to t\bar{t}$ is small. For the *no-Higgs* SM, the top quark event rate at LC is about half of that at the LHC and yields about 550 $t\bar{t}$ pair and single-t or $\bar{t}$ events. Again, we see that the $W_L^+W_L^- \to t\bar{t}$ rate is sensitive to the dimension 5 operators that correspond to X', but the $Z_LZ_L \to t\bar{t}$ rate is less sensitive [35]. Since the detection of the top quark at the LC would be easier than at the LHC (*i.e.* the detection efficiency would be larger), we conclude that the LC and the LHC can have the same sensitivity for probing the NLO fermionic operators via the $W_L^+W_L^- \to t\bar{t}$ process.

The production rates shown in figure 19 are for an unpolarized e^- beam at the LC. Assuming a longitudinally polarized e^- beam at the LC, the $W_L^+W_L^- \to t\bar{t}$ rate will be doubled because the coupling of the W boson to the electron is purely left handed so the parton luminosity of the W

---

[34] In $W_L^+Z_L \to t\bar{b}$, X_3 contributes to both, the S- and the P-partial waves.

[35] Needless to say, the $W_L^-Z_L$ rate is the same as the $W_L^+Z_L$ rate at an e^+e^- LC

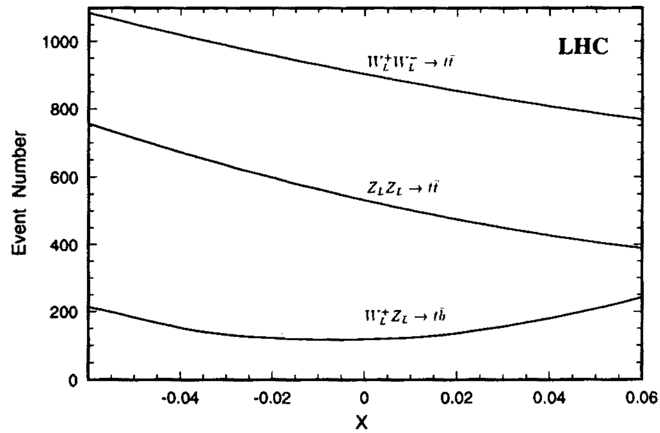

Fig. 18. Number of events at the LHC for $W_L^+W_L^-$, Z_LZ_L and $W_L^+Z_L$ fusion. The variable X stands for the effective coefficients X, X' and X_1 (Eqs (110), (112) and (114) respectively).

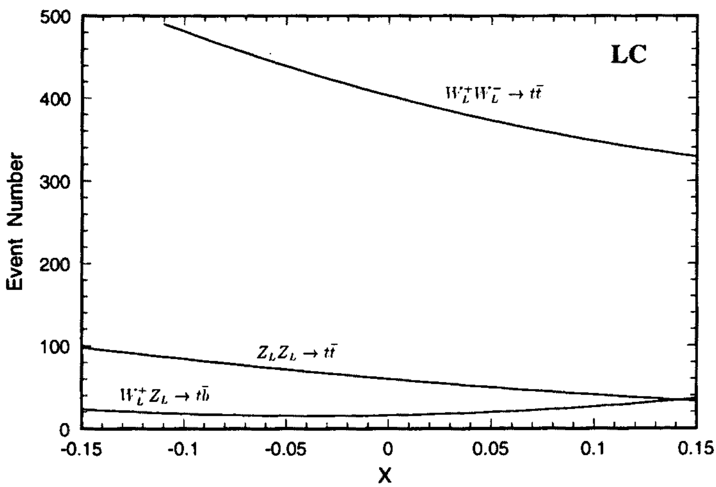

Fig. 19. Number of events at the LC for W_LW_L, Z_LZ_L and W_LZ_L fusion. The variable X stands for the effective coefficients X, X' and X_1 (Eqs. (110), (112) and (114) respectively).

from the electron beam will be doubled if this beam is polarized. However, this is not true for the parton luminosity of Z because in this case the Z-e-e coupling is nearly purely axial-vector $(1-4s_w^2 \approx 0)$ and the production rate of $Z_L Z_L \to t\bar{t}$ does not strongly depend on whether the electron beam is polarized or not. As shown in figure 19 , if the coefficient of the anomalous dimension 5 operators is as large as $0.1/\Lambda$ in magnitude then their effect can in principle [36] be identified in the measurement of $W_L^+ W_L^-$ fusion rate at the LHC and the LC. A similar conclusion also holds for the $Z_L Z_L$ and $W_L^\pm Z_L$ fusion processes with somewhat less sensitivity. It is useful to ask for the bounds on the coefficients of the anomalous dimension 5 operators if the measured production rate at the LHC and the LC is found to be in agreement with the *no-Higgs* SM predictions (*i.e.* with $X = 0$). At the 95% C.L. we summarize the bounds on the X's in Table IV. Here, only the statistical error is included. In practice, after including the branching ratios of the relevant decay modes and the detection efficiency of the events, these bounds will become somewhat weaker, but we do not expect an order of magnitude difference. Also, these bounds shall be improved by carefully analysing angular correlations when data is available.

TABLE IV

The range of parameters for which the total number of events deviates by less than 2σ from the *no-Higgs* SM prediction.

Process	LHC (pp)	LC (e^+e^-)
$W_L^{+(-)} Z_L \to t\bar{b}(b\bar{t})$	$-.035 < X_1 < .025$	$-.13 < X_1 < .07$
$W_L^{+(-)} Z_L \to t\bar{b}(b\bar{t})$	$-.045 < X_2 < .10$	$-.12 < X_2 < .35$
$W_L^{+(-)} Z_L \to t\bar{b}(b\bar{t})$	$-.19 < X_3 < .12$	$-.65 < X_3 < .35$
$W_L^+ W_L^- \to t\bar{t}$	$-.022 < X' < .017$	$-.06 < X' < .07$
$W_L^+ W_L^- \to t\bar{t}$	$-.11 < X_m < .06$	$-.28 < X_m < .13$
$Z_L Z_L \to t\bar{t}$	$-.015 < X < .017$	$-.07 < X < .08$

As shown in Table IV, these coefficients can be probed to about an order of 10^{-2} to 10^{-1}. For this Table, we have only consider an unpolarized e^- beam for the LC. To obtain the bounds we have set all the anomalous coefficients to be zero except the one of interest. (The definitions of the combined coefficients X, X', X_1, X_2 and X_3 are given in the previous section.)

If the LC is operated at the e^-e^- mode with the same CM energy of the collider, then it can not be used to probe the effects for $W_L^+ W_L^- \to t\bar{t}$, but it can improve the bounds on the combined coefficients X_1, X_2 and

[36] Of course, a complete study including signal versus background, detector efficiency, *etc.*, would be necessary in order to confirm this.

X_3 because the event rate will increase by a factor of 2 for $W_L^- Z_L \to b\bar{t}$ production.

By combining the limits of these ranges of parameters we can find the corresponding limits on the range of the effective coefficients a_{zz1}, a_{z2}, a_{z3}, a_{z4}, and a_m. For example, if we consider the limits for the LC, we will see that the limits for a_{z2} and a_{z3} are directly given by X_2 and X_3, respectively. Then, we can combine this information with the limits given for X' and X_m, to find the limits for a_{zz1} $(-.38 < a_{zz1} < .24)$ and for a_m $(-.34 < a_m < .3)$. If we consider one anomalous coupling at a time, then these bounds can be largely improved, for instance $-0.03 < a_{zz1} < 0.04$ from X' (for $W_L^+ W_L^- \to t\bar{t}$ scattering).

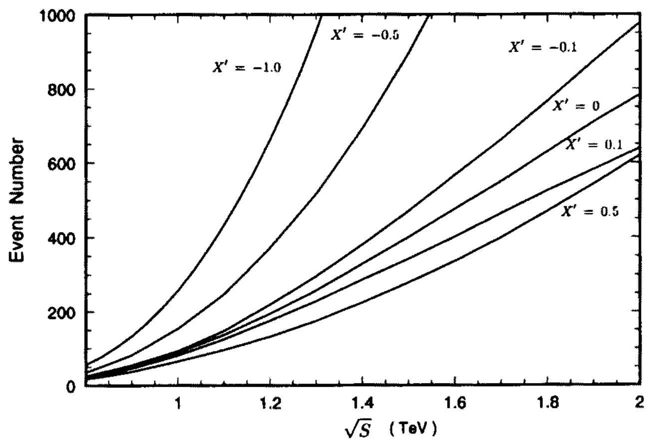

Fig. 20. Number of $t\bar{t}$ events at the LC from $W_L^+ W_L^-$ fusion for different values of the effective coefficient X' as a function of the CM energy.

The above results are for the LC with a 1.5 TeV CM energy. To study the possible new effects in the production rates of $W_L^+ W_L^- \to t\bar{t}$ at the LC with different CM energies $E = \sqrt{s}$ we plot the production rates for various values of X' in figure 20 (Again, $X' = 0$ stands for the *no-Higgs* SM). If X' can be as large as -1.0, then a 1 TeV LC will already observe the anomalous rate via $W_L^+ W_L^-$ fusion [37]. For $X' = 0.5$ the event rate at 1.5 TeV is down by about a factor of 2 from the SM event rate [38].

[37] If X' is too big , partial wave unitarity is violated at this order.

[38] For positive values of X' the rate tends to diminish below the SM rate, but then at some value near 0.5 the rate begins to grow back up towards the SM rate.

6.4. CP violating effects due to dimension 5 interactions

The complete set of anomalous dimension 5 operators listed in $\mathcal{L}^{(5)}$ consists of CP-invariant and CP-violating operators. In our study of the top quark production rates due to these anomalous operators up to order $1/\Lambda$, we have only considered the CP-even part of the operators. Their contribution, like the one from the *no-Higss* SM at tree level, is real. If the coefficient of the CP-violating part is not zero, then it will contribute to the imaginary part of the helicity amplitude, and one has to examine CP-odd observables to probe these operators.

To illustrate this point, let us consider the CP-odd part of the four-point scalar type operator O_{gWW} and the electric dipole moment term of $O_{\mathcal{A}}$ (Eqs. (92) and (87)). After including the contributions from the *no-Higss* SM and the above two CP-odd operators, the helicity amplitudes for the $W_L^+W_L^- \to t\bar{t}$ process in the $W_L^+W_L^-$ CM frame are:

$$\begin{aligned} a_{\pm\pm} &= \pm\frac{m_t E}{v^2} + i2\frac{E^3}{v^2}\frac{(\tilde{a}_{ww1} + 2a_d c_\theta)}{\Lambda}, \\ a_{+-} &= \frac{2\, {m_t}^2\, s_\theta}{\left(\frac{{m_b}^2}{2E^2} + (1-c_\theta)\left(1-\frac{{m_t}^2}{2E^2}\right)\right)v^2}, \\ a_{-+} &= 0\,, \end{aligned} \tag{115}$$

where by a_d and $\tilde{a}_{ww1}$ we refer to the imaginary parts of the coefficients of $O_{\mathcal{A}}$ and O_{gWW}, respectively.

One of the CP-odd observables that can measure a_d and $\tilde{a}_{ww1}$ is the transverse polarization $P_\perp$ of the top quark which is the degree of polarization of the top quark in the direction perpendicular to the plane of the $W_L^+W_L^- \to t\bar{t}$ scattering process.

It was shown in Ref. [70] that

$$P_\perp = \frac{2Im\,(a_{++}^* a_{-+} + a_{+-}^* a_{--})}{|ww_{++}|^2 + |ww_{+-}|^2 + |ww_{-+}|^2 + |ww_{--}|^2} \tag{116}$$

which gives, up to the order $1/\Lambda$,

$$P_\perp \cong \frac{4 s_\theta E}{\left(\frac{{m_b}^2}{2E^2} + (1-c_\theta)\left(1-\frac{{m_t}^2}{2E^2}\right)\right)} \frac{(\tilde{a}_{ww1} + 2a_d c_\theta)}{\Lambda}\,, \tag{117}$$

where $E = \sqrt{s}$ is the CM energy of the W^+W^- system, and $P_\perp$ is defined to be a value between -1 and 1. For instance, for $E = 1.5$ TeV, $\Lambda = 3$ TeV, and $\theta = \pi/2$ (or $\pi/3$), we obtain $P_\perp = 4\tilde{a}_{ww1}$ (or $4\sqrt{3}(\tilde{a}_{ww1} + a_d)$).

Since $P_\perp$ is bounded to be 1 by definition, this requires $\mid \tilde{a}_{ww1} \mid < 1/4$ and $\mid \tilde{a}_{ww1} + a_d \mid < 1/4\sqrt{3}$.

If we consider a 1.5 TeV e^+e^- collider with a number of $t\bar{t}$ events from $W_L^+W_L^-$ fusion of approximately 100 (which is approximately the *no-Higgs* SM rate for a W^+W^- invariant mass between 800 GeV and 1100 GeV) and assume that $P_\perp$ can be measured to about $1/\sqrt{100} = 10\%$, then an agreement between data and the *no-Higgs* SM prediction ($P_\perp = 0$ at tree level) implies that $\mid \tilde{a}_{ww1} \mid \leq 0.04$ for the case that $a_d = 0$.

7. Conclusions

Because top quark is heavy ($m_t \sim v/\sqrt{2}$), it is likely that the interaction of the top quark can deviate largely from the SM predictions if the electroweak symmetry breaking and the generation of fermion masses are closely related. In this study, we have applied the electroweak chiral Lagrangian to probe new physics beyond the SM by studying the couplings of the top quark to gauge bosons. We have restricted ourselves to only consider the interactions of the top and bottom quarks and not the flavor changing neutral current vertices like t-c-Z. Furthermore, seeing the heaviness of the top quark as a possible indication that any new physics effects associated to the symmetry breaking (and mass generating) sector will manifest themselves preferably on this particle, we have considered only the couplings that involve the top quark as showing possible deviations from the standard values. (The vertex b-b-Z is considered unmodified.) We introduced 4 effective coefficients: two that represent the non-standard couplings associated to the left and right handed charged currents κ_L^{CC} and κ_R^{CC}, and two more for the anomalous left and right handed neutral currents κ_L^{NC} and κ_R^{NC}. Then, we used the precision LEP data to set bounds on the couplings κ_L^{NC}, κ_R^{NC}, and κ_L^{CC}, and we also discussed how the SLC measurement of A_{LR} can modify these constraints. The right handed charged current coupling κ_R^{CC} has to be constrained by means of the CLEO measurement on $b \to s\gamma$. Last, we showed how to improve our knowledge about the top quark nonstandard couplings at current and future colliders such as at the Tevatron, the LHC, and the LC.

Because of the non-renormalizability of the electroweak chiral Lagrangian one can only estimate the size of these nonstandard couplings by studying the contributions to LEP/SLC observables at the order of $m_t^2 \ln \Lambda^2$, where $\Lambda = 4\pi v \sim 3$ TeV is the cutoff scale of the effective Lagrangian. Nevertheless, this does not mean we can not extract useful information. For instance, by assuming that the b-b-Z vertex is not modified, we found that κ_L^{NC} is already constrained to be $-0.05 < \kappa_L^{NC} < 0.17$ ($0.0 < \kappa_L^{NC} < 0.15$)

by LEP/SLC data at the 95% C.L. for a 160 (180) GeV top quark. Although $\kappa_{\rm R}^{\rm NC}$ and $\kappa_{\rm L}^{\rm CC}$ are allowed to be in the full range of ± 1, the precision LEP/SLC data do impose some correlations among $\kappa_{\rm L}^{\rm NC}$, $\kappa_{\rm R}^{\rm NC}$, and $\kappa_{\rm L}^{\rm CC}$. ($\kappa_{\rm R}^{\rm CC}$ does not contribute to the LEP/SLC observables of interest in the limit of $m_b = 0$.)

Inspired by the experimental fact $\rho \approx 1$, reflecting the existence of an approximate custodial symmetry, we related $\kappa_{\rm L}^{\rm NC}$ and $\kappa_{\rm L}^{\rm CC}$. Then, the remaining two free parameters $\kappa_{\rm L} = \kappa_{\rm L}^{\rm NC}$ and $\kappa_{\rm R} = \kappa_{\rm R}^{\rm NC}$ get to be strongly correlated as well ($\kappa_{\rm L} \sim 2\kappa_{\rm R}$).

We noted that the relations among the κ's can be used to test different models of electroweak symmetry-breaking. For instance, a heavy SM Higgs boson ($m_H \gg m_t$) will modify the couplings t-t-Z and t-b-W of a heavy top quark at the scale m_t such that $\kappa_{\rm L}^{\rm NC} = 2\kappa_{\rm L}^{\rm CC}$, $\kappa_{\rm L}^{\rm NC} = -\kappa_{\rm R}^{\rm NC}$, and $\kappa_{\rm R}^{\rm CC} = 0$. Another example is the effective model discussed in Ref. [2] where, $\kappa_{\rm R}^{\rm CC} = \kappa_{\rm L}^{\rm CC} = 0$, in which the low energy precision data impose the relation $\kappa_{\rm L} \sim \kappa_{\rm R}$. On the other hand, the simple commuting extended technicolor model presented in Ref. [9] predicts that the nonstandard top quark couplings are of the same order as the nonstandard bottom quark couplings, and are thus small.

Undoubtedly, direct detection of the top quark at the Tevatron, the LHC, and the LC is crucial to measuring the couplings of t-b-W and t-t-Z. At hadron colliders, $\kappa_{\rm L}^{\rm CC}$ and $\kappa_{\rm R}^{\rm CC}$ can be measured by studying the polarization of the W boson from top quark decay in $t\bar{t}$ events, and from the production rate of the single top quark event via W-gluon fusion, W^* or Wt processes. The LC is the best machine to measure $\kappa_{\rm L}^{\rm NC}$ and $\kappa_{\rm R}^{\rm NC}$ which can be measured from studying the angular distribution and the polarization of the top quark produced in e^-e^+ collision.

If a strong dynamics of the electroweak symmetry breaking mechanism can largely modify the dimension 4 anomalous couplings, it is natural to ask whether the same dynamics can also give large dimension 5 anomalous couplings. In the framework of the electroweak chiral Lagrangian, we have found that there are 19 independent dimension five operators associated with the top quark and the bottom quark system. The high energy behavior, two powers in E above the *no-Higgs* SM, for the $V_{\rm L}V_{\rm L} \to t\bar{t}$, $t\bar{b}$, (or $b\bar{t}$) processes, gives them a good possibility to manifest themselves through the production of $t\bar{t}$ pairs or single-t or $\bar{t}$ events at the LHC and LC in high energy collisions. Since in the high energy regime a longitudinal gauge boson is equivalent to the corresponding would-be Goldstone boson (cf. Goldstone Equivalence Theorem [21]), the production of top quarks via $V_{\rm L}V_{\rm L}$ fusions can probe the part of the electroweak symmetry breaking sector which modifies the top quark interactions. To simplify our discussion on the accuracy for the measurement of these anomalous couplings at future colliders, we have taken the dimension 4 anomalous couplings to be zero for this part of the study. Also we have considered a special class of new physics effects in which an underlying custodial SU(2) symmetry is assumed that gets broken in such a way as to keep the vertices of the bottom quark unaltered (as was done for the dimension 4 case). This approximate custodial symmetry then relates some of the coefficients of the anomalous operators. Then we study the contributions of these couplings to the production rates of the top quark. We find that for the leading contributions at high energies, only the S- and P-partial wave amplitudes are modified by these anomalous couplings if the magnitudes of the coefficients of the anomalous dimension 5 operators are allowed to be as large as 1 (as suggested by the naive dimensional analysis [24, 16]), then we will be able to make an unmistakable identification of their effects to the production rates of top quarks via the longitudinal weak boson fusions. However, if the measurement of the top quark production rate is found to agree with the SM prediction, then one can bound these coefficients to be at most of order 10^{-2} or 10^{-1}. This is about a factor $(\Lambda/m_t) \simeq 3$ TeV/175 GeV $\sim O(10)$ more stringent than in the case of the study of NLO bosonic operators via the $V_{\rm L}V_{\rm L} \to V_{\rm L}V_{\rm L}$ scattering processes [21, 22, 68]. Hence, for those models of electroweak symmetry breaking for which the naive dimensional analysis gives the correct size for the coefficients of dimension 5 effective operators, the top quark production via $V_{\rm L}V_{\rm L}$ fusions can be a more sensitive probe to EWSB than the longitudinal gauge boson pair production via $V_{\rm L}V_{\rm L}$ fusions which is commonly studied. For completeness, we also briefly discuss how to study the CP-odd operators by measuring the CP-odd observables. In this paper we study their effects on the transverse (relative to the plane of $W_{\rm L}^+W_{\rm L}^- \to t\bar{t}$ scattering) polarization of the top quark.

In conclusion, the production of top quarks via $V_{\rm L}V_{\rm L}$ fusions at the LHC and the LC should be carefully studied when data is available because it can be sensitive to the electroweak symmetry breaking mechanism, even more than the commonly studied $V_{\rm L}V_{\rm L} \to V_{\rm L}V_{\rm L}$ processes in some models of strong dynamics.

C.P.Y. would like to thank Marek Jezabek and all those involved in organizing the Cracow school for their warm hospitality. We thank Douglas Carlson and Hong-Jian He for helpful discussions. F. Larios was supported in part by the Organization of American States, and by the Sistema Nacional de Investigadores. C.P.Y. was supported in part by the NSF grants PHY-9309902 and PHY-9507683.

REFERENCES

[1] F. Abe *et al.*, *Phys. Rev. Lett.* **73**, 225 (1994); S. Abachi *et al.*, *Phys. Rev. Lett.* **72**, 2138 (1994).

[2] R.D. Peccei, S. Peris, X. Zhang, *Nucl. Phys.* **B349**, 305 (1990); T. Han, R.D. Peccei, X. Zhang, Fermilab-pub-95/160-T, 1995; E. Malkawi, T. Tait, MSUHEP-51116, 1995.

[3] R.S. Chivukula, E. Gates, E.H. Simmons, J. Terning, *Phys. Lett.* **B311**, 157 (1993); R.S. Chivukula, E.H. Simmons, J. Terning, *Phys. Lett.* **B331**, 383 (1994).

[4] E. Malkawi, C.–P. Yuan. *Phys. Rev.* **D50**, 4462 (1994).

[5] G.L. Kane, in Proceedings of the Workshop on High Energy Phenomenology, Mexico City, July 1–10, 1991.

[6] For a review see, H.E. Haber, SCIPP-91-06. Invited lectures given at Theoretical Advanced Study Inst. (TASI-90), Boulder, CO, Jun 3-29, 1990. Published in Boulder TASI 90:340-475 (QCD161:T45:1990)

[7] K. Lane, BUHEP-94-2. Lectures given at Theoretical Advanced Study Institute (TASI 93) in Elementary Particle Physics: The Building Blocks of Creation — From Microfermius to Megaparsecs, Boulder, CO, 6 Jun–2 Jul 1993. In Boulder 1993, Proceedings, The Building Blocks of Creation 381-408; and the references therein.

[8] R.S. Chivukula, E.H. Simmons, J. Terning, *Phys. Lett.* **B331**, 383 (1994).

[9] R.S. Chivukula, E. Gates, E.H. Simmons, J. Terning, *Phys. Lett.* **B311**, 157 (1993).

[10] Y. Nambu. In *Proc. of the 1988 International Workshop on New Trends in Strong Coupling Gauge Theories, Nagoya, Japan,* eds M. Bando, T. Muta, K. Yamawaki, World Scientific, Singapore 1989; W.A. Bardeen, C.T. Hill, M. Lindner, *Phys. Rev.* **D41**, 1647 (1990); R. Bönisch, A. Leike, DESY-93-111, hep-ph/9308346; B. A. Kniehl, A. Sirlin, *Phys. Rev.* **D51**, 3803 (1995).

[11] M. Chanowitz, M.K. Gillard, *Phys. Lett.* **B142**, 85 (1984); J. Bagger *et al.*, *Phys. Rev.* **D49**, 1246 (1994).

[12] H. Georgi, *Annu. Rev. Nucl. Part. Sci.* **43**, 209 (1993).

[13] M.A. Perez, J.J. Toscano, J. Wudka, *Phys. Rev.* **D 52**, 494 (1995); R. Martinez, M.A. Perez, J.J. Toscano, *Phys. Lett.* **B 340**, 91 (1994).

[14] *Physics of Top Quark at the Tevatron*, Talk given at the V Latinoamerican Workshop on Fundamental Interactions, Puebla, Mexico, Nov. 1995.

[15] S. Weinberg, *Physica* **96A**, 327 (1979); C.G. Callan, S. Coleman, J. Wess, B. Zumino, *Phys. Rev.* **D177**, 2247 (1969).

[16] H. Georgi, *Weak Interactions and Modern Particle Theory* The Benjamin/Cummings Publishing Company, 1984.

[17] R.N. Cahn, S. Dawson, *Phys. Lett.* **B136**, 196 (1984), *Phys. Lett.* **B138**, 464(E) (1984); M.S. Chanowitz, M.K. Gaillard, *Phys. Lett.* **B142**, 85 (1984); G.L. Kane, W.W. Repko, W.R. Rolnick, *Phys. Lett.* **B148**, 367 (1984); S. Dawson, *Nucl. Phys.* **B249**, 42 (1985); *Phys. Lett.* **B217**, 347 (1989); J. Lindfors, *Z. Phys.* **C28**, 427 (1985); W.B. Rolnick, *Nucl. Phys.* **B274**, 171 (1986); P.W. Johnson, F.I. Olness, W.–K. Tung, *Phys. Rev.* **D36**, 291 (1987); Z. Kunszt, D.E. Soper, *Nucl. Phys.* **B296**, 253 (1988); A. Abbasabadi, W.W. Repko, D.A. Dicus, R. Vega, *Phys. Rev.* **D38**, 2770 (1988); S. Cortese, R. Petronzio, *Phys. Lett.* **B276**, 203 (1992).

[18] J.M. Cornwall, D.N. Levin, G. Tiktopoulos, *Phys. Rev.* **D10**, 1145 (1974); C.E. Vayonakis, *Lett. Nuovo. Cimento* **17**, 383 (1976); B.W. Lee, C. Quigg, H. Thacker, *Phys. Rev.* **D16**, 1519 (1977); M.S. Chanowitz, M.K. Gaillard, *Nucl. Phys.* **B261**, 379 (1985); G.J. Gounaris, R. Kögerler, H. Neufeld, *Phys. Rev.* **D34**, 3257 (1986); H. Veltman, *ibid*, **D41** 2294 (1990); W.B. Kilgore, *Phys. Lett.* **B294**, 257 (1992).

[19] Y.-P. Yao, C.-P. Yuan, *Phys. Rev.* **D38**, 2237 (1988); J. Bagger, C. Schmidt, *Phys. Rev.* **D41**, 264 (1990).

[20] H.-J. He, Y.-P. Kuang, X. Li, *Phys. Rev. Lett.* **69**, 2619 (1992); *Phys. Rev.* **D49**, 4842 (1994); *Phys. Lett.* **B329**, 278 (1994); H.-J. He, W.B. Kilgore, DESY-96-079 and hep-ph/9609326 (*Phys. Rev.* **D**, in press).

[21] H.-J. He, Y.-P. Kuang, C.-P. Yuan, *Phys. Rev.* **D51**, 6463 (1995), and references therein; hep-ph/9503359, Published in Proc. International Symposium on *Beyond The Standard Model IV,* Page 610, Eds. J.F. Gunion, T. Han, J. Ohnemus, December 13-18, 1994, Tahoe, California, USA.

[22] H.-J. He, Y.-P. Kuang, C.-P. Yuan, *Phys. Lett.* **B382**, 149 (1996); hep-ph/9611316 (to appear in *Phys. Rev.* **D**; MSUHEP-51201, Published in Proc. of International Workshop on Physics and Experiments with Linear Colliders, September 8-12, 1995, Iwate, Japan, and in Proc. of Fermilab Linear Collider Workshop: Physics with High Energy e^+e^- Colliders, November 16-18, 1995, Batavia, USA.

[23] F. Larios, C.-P. Yuan, *Top Quark Interactions and the Search for New Physics.* MSUHEP-60620, hep-ph\9606397.

[24] A. Manohar, H. Georgi, *Nucl. Phys.* **B234**, 189 (1990).

[25] E. Malkawi, C.-P. Yuan, *Phys. Rev.* **D52**, 472 (1995).

[26] S. Coleman, J. Wess, Bruno Zumino, *Phys. Rev.* **D177**, 2239 (1969); C.G. Callan, S. Coleman, J. Wess, Bruno Zumino, *Phys. Rev.* **D177**, 2247 (1969).

[27] M. Chanowitz, M. Golden, H. Georgi. *Phys. Rev.* **D36**, 1490 (1987).

[28] F. Feruglio, *Int. J. Mod. Phys.* **A8**, 4937 (1993); and the references therein.

[29] T. Appelquist, G.-H. Wu, *Phys. Rev.* **D48**, 3241 (1993); and the references therein.

[30] R.D. Peccei, X. Zhang, *Nucl. Phys.* **B337**, 269 (1990).

[31] K. Fujikawa, A. Yamada, *Phys. Rev.* **D49**, 5890 (1994).

[32] M. Alam *et al.*, CLEO collaboration, *Phys. Rev. Lett.* **74**, 2885 (1995).

[33] R. Barbieri, IFUP–TH-23/93, July 1993, in *Lectures given at the Symposium on Particle Physics at the Fermi scale, Beijing, May 27 –June 4, 1993.* Published in CCAST Symposium 1993:163-212 (QCD161:S12:1993).

[34] G. Altarelli, R. Barbieri, F.Caravaglios, *Nucl. Phys.* **B405**, 3 (1993).

[35] G. Altarelli, R. Barbieri, *Phys. Lett.* **B253**, 161 (1990); G. Altarelli, R. Barbieri, S. Jadach, *Nucl. Phys.* **B369**, 3 (1992).

[36] G. Altarelli, CERN-TH/96-05. *Lectures presented at the Hellenic School on Elementary Particle Physics*, Corfu, Greece, Sep 3-11, 1995 and Rencontres du Vietnam, Ho Chi Minh City, Vietnam, Oct 21-24, 1995.

[37] G. Altarelli, R. Barbieri, F. Caravaglios, *Phys. Lett.* **B349**, 145 (1995).

[38] C.P. Burgess, D. London, *Phys. Rev.* **D48**, 4337 (1993).

[39] M.B. Einhorn, UM-TH-93-12. In Coral Gables 1993, Proceedings, Unified symmetry in the small and in the large, 407-420.

[40] H. Georgi, *Nucl. Phys.* **B361**, 339 (1991).

[41] G. Altarelli, CERN-TH-95/196; and the references therein.

[42] E. Malkawi, Ph.D. thesis, Michigan State University, August 1996; and the references therein.

[43] J.F. Donoghue, E. Golowich, B.R. Holstein, *Dynamics of the Standard Model* Cambridge Monographs on Particle Physics, Nuclear Physics and Cosmology, Cambridge University Press, 1992.

[44] M. Veltman, *Nucl. Phys.* **B123**, 89 (1977).

[45] P. Langacker, hep-ph/9412361, to be published in *Precision Tests of the Standard Electroweak Model*, ed. P. Langacker, World Scientific, Singapore 1994.

[46] The SLD Collaboration, K. Abe *et al.*, *Phys. Rev. Lett.* **73**, 25 (1994).

[47] S. Dawson, *Nucl. Phys.* **B249**, 42 (1985); S. Dawson, S. Willenbrock, *Nucl. Phys.* **B284**, 449 (1987); S. Willenbrock, D.A. Dicus, *Phys. Rev.* **D34**, 155 (1986); F. Anselmo, B. van Eijk, G. Bordes, *Phys. Rev.* **D45**, 2312 (1992); T. Moers, R. Priem, D. Rein, H. Reithler, in *Proceedings of Large Hadron Collider Workshop*, preprint CERN 90-10, 1990; R.K. Ellis, S. Parke, *Phys. Rev.* **D46**, 3785 (1992).

[48] C.–P. Yuan, *Phys. Rev.* **D41**, 42 (1990); D. Carlson, C.–P. Yuan, *Phys. Lett.* **B306**, 386 (1993).

[49] S. Cortese, R. Petronzio, *Phys. Lett.* **B253**, 494 (1991).

[50] D.O. Carlson, Ph.D. thesis, Michigan State University, MSUHEP-050727, August 1995; and the references therein.

[51] T. Stelzer, S. Willenbrock, *Phys. Lett.* **B374**, 169 (1996).

[52] G.A. Ladinsky, C.–P. Yuan, *Phys. Rev.* **D43**, 789 (1991);

[53] C.–P. Yuan, *et al.*, *Report of the subgroup on the Top Quark*, Proceedings of Workshop on Physics at Current Accelerators and Supercolliders, eds J. Hewett, A. White and D. Zeppenfeld, 1993, pp 495–505; and the references therein.

[54] Future Electro Weak Physics at the Fermilab Tevatron, eds D. Amidei, R. Brock, *Report of the tev_2000 study group.* Fermilab-Pub-96/082 (1996).

[55] G. L. Kane, G. A. Ladinsky, C.–P. Yuan, *Phys. Rev.* **D45**, 124 (1992).

[56] S. Mrenna, C.–P. Yuan, *Phys. Rev.* **D46**, 1007 (1992).

[57] P.W. Johnson, F.I. Olness, W.–K. Tung, *Phys. Rev.* **D36**, 291 (1987); and the references therein.

[58] The CDF Collaboration and J. Incandela, *CDF Top Quark Production and Mass*, FERMILAB–CONF–95/237–E, July 1995.

[59] J.C. Collins, W.–K. Tung, *Nucl. Phys.* **B278**, 934 (1986); F. Olness, W.–K. Tung, *Nucl. Phys.* **B308**, 813 (1988); M. Aivazis, F. Olness, W.–K. Tung, *Phys. Rev. Lett.* **65**, 2339 (1990); *Phys. Rev.* **D50**, 3085 (1994); M. Aivazis, J.C. Collins, F. Olness, W.–K. Tung, *Phys. Rev.* **D50**, 3102 (1994).

[60] G. Bordes, B. van Eijk, *Nucl. Phys.* **B435**, 23 (1995).

[61] J. Botts, J. Huston, H. Lai, J. Morfin, J. Owens, J. Qiu, W.-K. Tung, H. Weerts, Michigan State University preprint MSUTH-93/17.

[62] G. Bordes, B. Van Eijk, *Nucl. Phys.* **B435**, 23 (1995).

[63] A. Castro, The CDF Collaboration, FERMILAB-CONF-96/319-E. Published in Proceedings 28th International Conference on High Energy Physics (ICHEP'96), Warsaw, Poland, July 25-31, 1996.

[64] M. Smith, S. Willenbrock, hep-ph/9604223.

[65] G.A. Ladinsky, C.–P. Yuan, *Phys. Rev.* **D49**, 4415 (1994).

[66] T. Barklow, C.R. Schmidt, SCIPP 94/22, Aug 1994.

[67] W. Buchmüller, D. Wyler, *Nucl. Phys.* **B268**, 621 (1986).

[68] J. Bagger, V. Barger, K. Cheung, J. Gunion, T. Han, G.A. Ladinsky, R. Rosenfeld, C.-P. Yuan, *Phys. Rev.* **D49**, 1 (1994); **D52**, 3878 (1995); V. Barger, J.F. Beacom, K. Cheung, T. Han, *Phys. Rev.* **D50**, 6704 (1993).

[69] H.L. Lai, J. Botts, J. Huston, J.G. Morfin, J.F. Owens, J.W. Qiu, W.–K. Tung, H. Weerts, *Phys. Rev.* **D51**, 4763 (1995).

[70] G. Kane, G.A. Ladinsky, C.–P. Yuan, *Phys. Rev.* **D45**, 124 (1992).